2010

Financial Securities Under Nonlinear Diffusion Asset Pricing Model

Andrey Vasilyev
Wilfrid Laurier University

Your file Votre référence
ISBN: 978-0-494-68706-2
Our file Notre référence
ISBN: 978-0-494-68706-2

FINANCIAL SECURITIES UNDER NONLINEAR DIFFUSION ASSET PRICING MODELS

by

ANDREY VASILYEV

BSc in Mathematics, Belarussian State University, Minsk, Belarus, 2006

THESIS

Submitted to the Department of Mathematics, Faculty of Science

in partial fulfilment of the requirements for

MASTER OF SCIENCE

Wilfrid Laurier University

2010

Abstract

In this thesis we investigate two pricing models for valuing financial derivatives. Both models are diffusion processes with a linear drift and nonlinear diffusion coefficient. The forward price process of these models is a martingale under an assumed risk-neutral measure and the transition probability densities are given in analytically closed form. Specifically, we study and calibrate two different families of models that are constructed based on a so-called diffusion canonical transformation. One family follows from the Ornstein–Uhlenbeck diffusion (the UOU family) and the other – from the Cox–Ingersoll–Ross process (the Confluent–U family).

The first part of the thesis considers single-asset and multi-asset modeling under the UOU model. By applying a Gaussian copula, a multivariate UOU model is constructed whereby all discounted asset (forward) prices are martingales. We succeed in calibrating the UOU model to market call option prices for various companies. Moreover, the multivariate UOU model is calibrated to historical return data and captures the correlations for a pool of 4 assets.

In the second part of the thesis we examine the application of the Confluent-U model to the credit risk modeling. An equity-based structural first-passage time default model is constructed based on the Confluent-U model with efficient closed-form (i.e. spectral expansions) formulas for default probabilities. The model robustness is tested by its calibration to the credit default swap (CDS) spreads for companies with various credit ratings. It is shown that the model can be accurately calibrated to the credit spreads with a piecewise default barrier level. Finally, we investigate the linkage between CDS spreads and out-of-the-money put options.

Acknowledgements

I would like to thank all people who made this possible. I wish to express my sincere appreciation to Dr. Roman Makarov for his time, effort and guidance on this study. I am especially thankful to Dr. Joe Campolieti for his advice, encouragement, support, and guidance as a teacher and supervisor throughout my graduate experience at Wilfrid Laurier University. A special acknowledgement is dedicated to SHARCNET (the Shared Hierarchical Academic Research Computing Network) for providing research resources and graduate scholarship.

Table of Contents

Introduction

Diffusion processes are widely used in financial modeling. The first application of diffusions for continuous-time asset pricing dates back to 1900 in the doctoral thesis by French mathematician Louis Bachelier [1], who implemented Brownian motion with drift as a model for asset price dynamics. To circumvent the problem of negative asset prices, geometric Brownian motion (GBM) soon became a standard model for stock price dynamics and other financial assets. The GBM model attracted attention in 1965 [2], when economist Paul Samuelson rediscovered Bachelier's thesis. The GBM model has a number of advantages. It admits analytically tractable transition probability density functions. Moreover, the discounted price process obeys the martingale property in a risk-neutral measure. In a arbitrage-free asset pricing framework, these probabilistic properties lead to closed-form pricing formulas for various financial derivatives. However, the GBM model fails to explain certain empirical properties of asset returns and financial derivatives. For instance, observed implied volatility surfaces of major stock markets exhibit various volatility smiles and skews, while the standard GBM model assumes constant local volatility. Consequently, such and other important market observations have led to the development of a variety of pricing models based on alternative stochastic processes.

Numerous model extensions introduced in recent years capture the phenomenon of volatility smiles. There exist stochastic volatility models (see [3] and [4]), where the volatility of the stock is assumed to be a mean reverting diffusion process, typically correlated with the stock process itself. The jump-diffusion models, originally suggested by Merton [5], generate volatility skews and smiles by adding discontinuous jumps to the diffusion dynamics (e.g., see [6], [7]). Another approach, which has been examined by many authors ([8]– [9]), allows the stock volatility to be a function of the stock price, resulting in local or state-dependent volatility diffusion models. Nonlinear state dependent models provide a richer and more flexible theoretical calibration framework for fitting implied volatility surfaces and option values to the observed market data.

In this thesis, we study and calibrate recently developed multi-parameter state dependent nonlinear volatility models, which are constructed based on a so-called diffusion canonical transformation methodology (see [10], [11]). By construction, the underlying asset price dynamics is not assumed to follow geometric Brownian motion, but rather we define the local volatility to be a *nonlinear* function of the underlying asset price.

The diffusion canonical transformation is essentially a combination of a change of probability measure together with a nonlinear mapping of an underlying diffusion process. While

the diffusion canonical transformation approach is applicable to a wide variety of underlying processes, in this thesis we specialize in two separate sets of applications using subfamilies of models that arise from either an underlying Ornstein–Uhlenbeck diffusion (the UOU family) or from the Cox–Ingersoll–Ross process (the Confluent-U family).

In particular, pricing and calibration of European-style options is considered under a new multivariate UOU model. The model was recently introduced by Campolieti, Makarov and Vasilyev in [12]. Each (univariate) stock price process is modeled as a UOU diffusion with four positive freely adjustable parameters, as well as with the drift parameter. For all choices of model parameters, the discounted UOU process is a martingale. Each choice gives a risk-neutral measure with the transition probability density function given in analytically closed form. The multivariate UOU process is then constructed by using a Gaussian copula function, where independent Ornstein–Uhlenbeck processes are coupled by employing a bridge copula method. The model is calibrated to a finite set of observed option prices via nonlinear least squares with a regularization method based on relative entropy with respect to a historical prior measure.

The second part of the thesis considers the so-called Confluent–U model. In particular, we examine its applicability to credit default and to pricing credit derivatives. The structural first-passage time default model is constructed based on the Confluent–U model with efficient closed-form formulas for default probabilities. We demonstrate how to construct an intensity based default model and also derive pricing formulas for bond spreads and credit default swap (CDS) spreads. The model robustness is tested by calibrating it to CDS spreads for companies with various credit ratings. Finally, we attempt to identify the linkage between CDS spread and out of the money put options as source of protection from credit default.

This thesis is organized as follows. In Chapter 1, we present the diffusion canonical transformation technique for generating transformed diffusions. In Chapter 2, we construct the multivariate UOU model and apply it to option pricing. Also, we present a step-by-step algorithm for calibrating the model to single-asset equity option market prices, as well as, a calibration algorithm of the multi-asset price correlation matrix to the historical asset prices. In Chapter 3 we construct a structural first-passage time default model based on the Confluent–U family. We also demonstrate how to price and calibrate the model to credit derivatives. We end with a concluding discussion.

1 Nonlinear Diffusion Pricing Models

1.1 Diffusion Canonical Transformation

Consider a diffusion process $(S_t)_{t\geq 0}$, started at S_0, with linear drift coefficient rS and nonlinear state dependent diffusion coefficient $\sigma(S)$, defined by the time-homogeneous stochastic differential equation (SDE)

$$\mathrm{d}S_t = rS_t\mathrm{d}t + \sigma(S_t)\mathrm{d}W_t\,, \tag{1.1}$$

where $(W_t)_{t\geq 0}$ is a standard Brownian motion. Considering applications to financial modeling, S_t may refer to the stock or asset price at calendar time t. S_t can also represent other processes such as a forward or instantaneous short interest rate. Throughout this thesis, S_t is defined on the real interval $\mathcal{D} = (0, \infty)$ and represents a stock price. As is shown originally for the zero drift case in [10], the diffusion canonical transformation methodology allows us to construct analytically solvable S-diffusions with state dependent volatility from simpler underlying X-diffusion processes by applying a combination of a monotonic map and a change of measure. The more general method which includes the case of affine drift is discussed in [13], [14].

Consider a one-dimensional time-homogeneous diffusion $(X_t^{(\rho)})_{t\geq 0} \in \mathcal{I} \subset \mathbb{R}$, with infinitesimal generator

$$\mathcal{G}^{(\rho)}f(x) := \frac{1}{2}\nu(x)^2 f''(x) + \left(\lambda(x) + \nu^2(x)\frac{\hat{u}'_\rho(x)}{\hat{u}_\rho(x)}\right) f'(x)\,, \tag{1.2}$$

$\hat{u}'_\rho(x) = \mathrm{d}\hat{u}_\rho(x)/\mathrm{d}x$, with $\hat{u}_\rho$ defined in (1.6), where $\rho > 0$ is a positive constant, $\lambda(x)$

and $\nu(x) > 0$, with continuous derivatives $\lambda'(x), \nu'(x), \nu''(x)$ on $\mathcal{I}$, are drift and diffusion coefficients. Such an $X^{(\rho)}$-diffusion can be viewed as arising from an underlying X-diffusion defined below by the application of a measure change, or a Doob h-transform with $h = \hat{u}_\rho$ (e.g. see [15], [10]).

The X-diffusion is started at x_0 and has SDE

$$\mathrm{d}X_t = \lambda(X_t)\mathrm{d}t + \nu(X_t)\mathrm{d}W_t\,, \tag{1.3}$$

with transition PDF $p_X(t; x_0, x)$. The regular diffusion $(X_t)_{t\geq 0}$ can also be defined by the respective scale and speed density functions [16]:

$$\mathfrak{s}(x) = \exp\left(-\int^x \frac{2\lambda(z)}{\nu^2(z)}\mathrm{d}z\right) \quad \text{and} \quad \mathfrak{m}(x) = \frac{2}{\nu^2(x)\mathfrak{s}(x)}\,, \tag{1.4}$$

with generator

$$\mathcal{G}f(x) \equiv \frac{1}{2}\nu^2(x)f''(x) + \lambda(x)f'(x)\,. \tag{1.5}$$

The generating function $\hat{u}_\rho(x)$ in (1.2) is a linear combination of the two fundamental solutions $\varphi_\rho^\pm$ of the the ordinary differential equation $\mathcal{G}\varphi_\rho^\pm = \rho\varphi_\rho^\pm$, where

$$\hat{u}_\rho(x) = q_1\varphi_\rho^+(x) + q_2\varphi_\rho^-(x)\,, \tag{1.6}$$

with parameters $q_1, q_2 \geq 0$ and at least one of them being strictly positive: $q_1 + q_2 > 0$. For $\rho > 0$, φ_ρ^+ and φ_ρ^- are then respectively strictly increasing and decreasing convex functions on $\mathcal{I}$. The transition PDF $p_X^{(\rho)}$ of the transformed process $X_t^{(\rho)}$ is related to the PDF p_X of X_t by

$$p_X^{(\rho)}(t; x_0, x) = e^{-\rho t}\frac{\hat{u}_\rho(x)}{\hat{u}_\rho(x_0)}p_X\left(t; x_0, x\right),\ x, x_0 \in \mathcal{I},\, t > 0\,. \tag{1.7}$$

The second part of the diffusion canonical transformation gives the S-process, with SDE (1.1), by applying a strictly monotonic real-valued map $\mathsf{F} : \mathcal{I} \to \mathcal{D}$ to an $X^{(\rho)}$-process: $S_t = \mathsf{F}(X_t^{(\rho)})$, where

$$|\mathsf{F}'(x)| = \frac{\sigma(\mathsf{F}(x))}{\nu(x)}\,. \tag{1.8}$$

The transition PDF for an S-diffusion is related to the transition PDFs of the X and $X^{(\rho)}$ diffusions as follows:

$$p_S(t;S_0,S)=\frac{\nu(x)}{\sigma(S)}\,p_X^{(\rho)}(t;x_0,x)=\frac{\nu(x)}{\sigma(S)}\frac{\hat{u}_\rho(x)}{\hat{u}_\rho(x_0)}e^{-\rho t}p_X\,(t;x_0,x)\;, \tag{1.9}$$

where $x=\mathsf{X}(S)$, $x_0=\mathsf{X}(S_0)$, and $\mathsf{X}:=\mathsf{F}^{-1}$ is the unique inverse of the mapping function F. The mapping function F has the following general quotient form [14]:

$$\mathsf{F}(x)=\frac{c_1\varphi^+_{\rho+r}(x)+c_2\varphi^-_{\rho+r}(x)}{q_1\varphi^+_\rho(x)+q_2\varphi^-_\rho(x)}=\frac{\hat{v}_{\rho+r}(x)}{\hat{u}_\rho(x)}\,, \tag{1.10}$$

where $c_1,c_2,q_1,q_2\in\mathbb{R}$, $\rho,\rho+r>0$ are real parameters such that

$$W[\hat{u}_\rho,\hat{v}_{\rho+r}](x):=u_\rho v'_{\rho+r}-u'_\rho\hat{v}_{\rho+r}\neq 0\,. \tag{1.11}$$

Various choices of underlying X-diffusions lead to several families of S-diffusions, such as Bessel, Ornstein–Uhlenbeck, Confluent hypergeometric models that are studied in [15] – [12].

As was mentioned earlier, the diffusion canonical transformation generates nonlinear state dependent volatility diffusion models. From equation (1.8) the volatility function has the following general representation (with $x=\mathsf{X}(S)$):

$$\begin{aligned}\sigma(S)=\sigma(\mathsf{F}(x))&=\nu(x)|\mathsf{F}'(x)|=\nu(x)\left|\frac{\hat{v}'_{\rho+r}(x)\hat{u}_\rho(x)-\hat{u}'_\rho(x)\hat{v}_{\rho+r}(x)}{\hat{u}^2_\rho(x)}\right|\\&=\nu(x)\frac{|W[\hat{u}_\rho,\hat{v}_{\rho+r}](x)|}{\hat{u}^2_\rho(x)}\,,\end{aligned} \tag{1.12}$$

where W denotes the Wronskian and given by (1.11).

1.2 Pricing European Vanilla Options

Consider an asset (i.e., a stock) price process $(S_t)_{t\geq 0}$ modeled as a diffusion according to (1.1). We note that for stocks that pay a dividend q then $r\longrightarrow r-q$ in (1.1). As is shown in [13] and [14], for specific choices of the underlying process (X_t) and parameters c_1,c_2,q_1,q_2, by applying the diffusion canonical transformation one can obtain S-diffusion families with

discounted process $(e^{-rt}S_t)_{t\geq 0}$ obeying the martingale property for every choice of model parameters. Hence, under the risk neutral valuation, choosing the money-market account as numeraire, the value of a European-style option is given by the conditional expectation under a risk-neutral probability measure $\mathbb{Q}$:

$$V(S_0,T) = e^{-rT}\mathbb{E}^{\mathbb{Q}}[\Lambda(S_T) \mid S_0] = e^{-rT}\mathbb{E}^{\mathbb{Q}}[\Lambda(\mathsf{F}(X_T^{(\rho)})) \mid X_0^{(\rho)} = \mathsf{X}(S_0)]\,, \tag{1.13}$$

where $\Lambda(S_T)$ is a payoff function. The option price of a standard European contract with payoff Λ can be written in terms of a one-dimensional integral as follows:

$$\begin{aligned} V(S_0,T) &= e^{-rT}\int_0^\infty p_S(T;S_0,S)\Lambda(S)\,\mathrm{d}S \\ &= \frac{e^{-(r+\rho)T}}{\hat{u}_\rho(x_0)}\int_{\mathcal{I}} \hat{u}_\rho(x)\,p_X(T;x_0,x)\Lambda(\mathsf{F}(x))\,\mathrm{d}x\,. \end{aligned} \tag{1.14}$$

As an example, let us consider a European call option that gives the holder the right to buy the underlying asset with current spot price S_0 at a certain date T for a certain strike price K. The payoff from a long position in a European call option is $\Lambda(S_T) = (S_T - K)^+$, where S_T is the asset price at expiration time T. Then according to equation (1.14), the European call option has value

$$\begin{aligned} V(S_0,T) &= e^{-rT}\mathbb{E}^{\mathbb{Q}}\left[\Lambda(S_T)\right] = e^{-rT}\mathbb{E}^{\mathbb{Q}}\left[\Lambda(\mathsf{F}(X_T^{(\rho)}))\right] \\ &= e^{-rT}\mathbb{E}^{\mathbb{Q}}\left[(\mathsf{F}(X_T^{(\rho)}) - K)\mathbf{1}_{\left\{\mathsf{F}(X_T^{(\rho)})\geq K\right\}}|X_0^{(\rho)} = x_0\right] \\ &= e^{-rT}\mathbb{E}^{\mathbb{Q}}\left[(\mathsf{F}(X_T^{(\rho)}) - K)\mathbf{1}_{\left\{X_T^{(\rho)}\geq \mathsf{X}(K)\right\}}|X_0^{(\rho)} = x_0\right] \\ &= \frac{e^{-(r+\rho)T}}{\hat{u}_\rho(x_0)}\int_{\mathsf{X}(K)}^{\infty} \hat{u}_\rho(x)\,p_X(T;x_0,x)(\mathsf{F}(x) - K)\,\mathrm{d}x\,, \end{aligned} \tag{1.15}$$

assuming that $\mathcal{I}$ is of the form (l,∞) and F is an increasing map.

2 Multi-Asset Option Pricing under the Ornstein–Uhlenbeck Family of Models

2.1 The UOU Family of Models

Consider the well-known Ornstein–Uhlenbeck (OU) process $(X_t)_{t\geq 0} \in \mathcal{I} \equiv (-\infty, \infty)$ having linear SDE

$$dX_t = (\lambda_0 - \lambda X_t)dt + \nu dW_t, \quad t > 0, \tag{2.1}$$

where λ_0, λ, ν are positive constants and $(W_t)_{t\geq 0}$ is a standard Brownian motion. Both left and right boundaries $l = -\infty$ and $r = \infty$ of the state space $\mathcal{I}$ are non-attracting natural for all choices of parameters. For simplicity, we set $\lambda_0 = 0$. The original process can be obtained by a linear shift $x \to x - \frac{\lambda_0}{\lambda}$ and $x_0 \to x_0 - \frac{\lambda_0}{\lambda}$. The speed and scale densities are

$$\mathfrak{s}(x) = e^{\kappa x^2/2} \quad \text{and} \quad \mathfrak{m}(x) = \frac{2}{\nu^2} e^{-\kappa x^2/2}, \tag{2.2}$$

where $\kappa := \frac{2\lambda}{\nu^2}$. The transition PDF of the regular OU process on $\mathbb{R}$ is given by

$$p_X(t; x_0, x) = \sqrt{\frac{\kappa}{2\pi(1 - e^{-2\lambda t})}} \exp\left(-\frac{\kappa(x - x_0 e^{-\lambda t})^2}{2(1 - e^{-2\lambda t})}\right). \tag{2.3}$$

Applying the diffusion canonical transformation framework of Section 1.1 to the underlying process $(X_t)_{t\geq 0}$ with the choice of $q_1 = 0, q_2 = 1, c_1 = a_0 > 0$, one obtains the unbounded Ornstein–Uhlenbeck (UOU) family of models. The generating function $\hat{u}_\rho(x)$ in this case is taken to be

$$\hat{u}_\rho(x) = e^{\kappa x^2/4} \mathcal{D}_{-\upsilon}(\sqrt{\kappa} x), \tag{2.4}$$

where $\upsilon \equiv \frac{\rho}{\lambda} > 0$ and $\mathcal{D}_{-\upsilon}(x)$ is Whittacker's parabolic cylinder function which is given in terms of confluent hypergeometric functions, see [17] for details. The fundamental solutions are now:

$$\varphi_\rho^-(x) = \exp\left(\frac{\kappa x^2}{4}\right)\mathcal{D}_{-\upsilon}(x\sqrt{\kappa}) \quad \text{and} \quad \varphi_\rho^+(x) = \varphi_\rho^-(-x). \tag{2.5}$$

Then according to equation (1.10) the mapping function is

$$\mathsf{F}(x) = a_0 \frac{\mathcal{D}_{-\upsilon - r/\lambda}(-x\sqrt{\kappa})}{\mathcal{D}_{-\upsilon}(x\sqrt{\kappa})}. \tag{2.6}$$

The above construction leads to an S-diffusion with volatility function (1.12) of the form:

$$\sigma(S) = a_0\sqrt{\kappa}\nu\left((\upsilon + \frac{r}{\lambda})\frac{\mathcal{D}_{-\upsilon-1-\frac{r}{\lambda}}(-\sqrt{\kappa}x)}{\mathcal{D}_{-\upsilon}(\sqrt{\kappa}x)} + \upsilon\frac{\mathcal{D}_{-\upsilon-\frac{r}{\lambda}}(-\sqrt{\kappa}x)\mathcal{D}_{-\upsilon-1}(\sqrt{\kappa}x)}{\mathcal{D}^2_{-\upsilon}(\sqrt{\kappa}x)}\right), \tag{2.7}$$

where $x = \mathsf{X}(S) = \mathsf{F}^{-1}(S)$. The volatility function $\sigma(S)$ depends on various adjustable positive parameters $\xi = \{a_0, \lambda, \kappa, \rho\}$ and drift rate r. It is important to notice that for the driftless case with $r = 0$, formula (2.7) reduces to

$$\sigma(S) = \sigma(\mathsf{F}(x)) = \frac{a_0\nu w_\rho \mathfrak{s}(x)}{\hat{u}^2_\rho(x)} = \frac{a_0\nu w_\rho}{\mathcal{D}^2_{-\upsilon}(\sqrt{\kappa}x)}, \tag{2.8}$$

where $w_\rho = \frac{\sqrt{2\kappa\pi}}{\Gamma(\upsilon)}$ is a Wronskian constant. As seen in Figure 2.1, the curves for the local volatility function $\sigma(S)/S$ generated by formula (2.7) have a pronounced smile-like pattern.

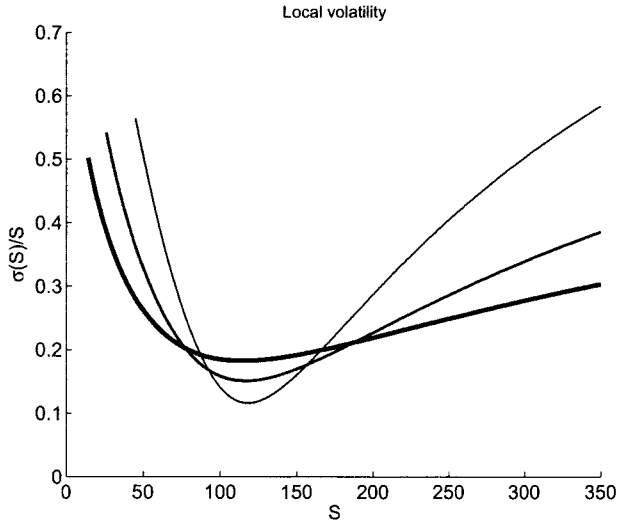

Figure 2.1: Local volatility function $\sigma(S)/S$ for the UOU family. The curves are plotted using model parameters $\xi = \{150, 0.125, 0.5, 0.01\}$ (the thinnest line), $\xi = \{150, 0.07, 0.5, 0.01\}$ (the moderate line), $\xi = \{150, 0.04, 0.5, 0.01\}$ (the thickest line) and $r = 0.02$.

As is shown in [11], [14] the discounted UOU process $(e^{-rt}S_t)_{t\geq 0}$ is a martingale for every choice of model parameters ξ. The transition density of the UOU process can be obtained from equation (1.9) and has the following representation:

$$p_S(t;S_0,S) = \frac{e^{-\rho t+\kappa(x^2-x_0^2)/4}}{a_0\mathcal{W}(x)}\frac{\mathcal{D}^3_{-\upsilon}(x\sqrt{\kappa})}{\mathcal{D}_{-\upsilon}(x_0\sqrt{\kappa})}p_X(t;x_0,x)\,, \tag{2.9}$$

where $x = \mathsf{X}(S)$, $x_0 = \mathsf{X}(S_0)$, $\mathcal{W}(x) = W[\mathcal{D}_{-\upsilon}(x\sqrt{\kappa}), \mathcal{D}_{-\upsilon-r/\lambda}(-x\sqrt{\kappa})] > 0$. For the $X^{(\rho)}$-diffusion, the transition PDF is given by substituting (2.3) into (1.7):

$$\begin{aligned} p_X^{(\rho)}(t;x_0,x) &= e^{-\rho t+\kappa(x^2-x_0^2)/4}\frac{\mathcal{D}_{-\upsilon}(x\sqrt{\kappa})}{\mathcal{D}_{-\upsilon}(x_0\sqrt{\kappa})}p_X(t;x_0,x) \\ &= e^{-\rho t+\kappa(x^2-x_0^2)/4}\frac{\mathcal{D}_{-\upsilon}(x\sqrt{\kappa})}{\mathcal{D}_{-\upsilon}(x_0\sqrt{\kappa})}\sqrt{\frac{\kappa}{2\pi(1-e^{-2\lambda t})}}\exp\left(-\frac{\kappa(x-x_0e^{-\lambda t})^2}{2(1-e^{-2\lambda t})}\right). \end{aligned} \tag{2.10}$$

2.2 Simulation of a Multi-Asset Price Process

2.2.1 Coupling UOU Processes

Consider a multi-asset price process $(\mathbf{S}_t)_{t\geq 0}$ with $\mathbf{S}_t \equiv (S_t^1,\ldots,S_t^n)$, where each individual asset price process $(S_t^k)_{t\geq 0}$, $k = 1,2,\ldots,n$, is modeled using a UOU diffusion model with SDE following (1.1) with common drift parameter r and diffusion function $\sigma = \sigma^k$. Hence, each of the n univariate processes is described by its own set of positive parameters $\xi_k = \{\lambda_k,\nu_k,a_{0,k},\rho_k\}$, $k = 1,2,\ldots,n$. Let the kth asset price process be described by the risk-neutral transition PDF of the form (2.9) with diffusion coefficient given by (2.7).

Following that notation, F^k and X^k will respectively denote the mapping function and its inverse function for the k-th asset. The transition PDFs p_X^k and $p_X^{(\rho_k,k)}$ are obtained from the kth underlying diffusion $(X_t^k)_{t\geq 0}$ and the transformed diffusion $\left(X_t^{(\rho_k,k)}\right)_{t\geq 0}$, respectively, for each $k = 1,\ldots,n$. Then the processes $(S_t^k)_{t\geq 0}$, $k = 1,2,\ldots,n$, are defined by

$$S_t^k = \mathsf{F}^k(X_t^{(\rho_k,k)})\,, \tag{2.11}$$

with the mapping F^k given by (2.6) and where $(X_t^{(\rho_k,k)})_{t\geq 0}$ has transition PDF (2.10) with parameters $\lambda = \lambda_k$, $\nu = \nu_k$, and $\rho = \rho_k$. The vector process $\mathbf{X}_t^{(\boldsymbol{\rho})} = \left(X_t^{(\rho_1,1)}, \ldots, X_t^{(\rho_n,n)}\right)$ denotes the n-variate process, and $(\mathbf{S}_t)_{t\geq 0}$ is obtained by applying the respective mapping function to each univariate diffusion: $S_t^k = \mathsf{F}^k\left(X_t^{(\rho_k,k)}\right)$, $k = 1, \ldots, n$. To specify a joint transition distribution function with given marginal distributions and a correlation structure we employ a copula function in what follows.

2.2.2 Copula Function

A copula $\mathcal{C}(u_1, u_2, \ldots, u_n)$, $u_k \in [0,1]$, $k = 1, \ldots, n$, is a multivariate CDF that links univariate marginal CDFs to their full multivariate distribution (for a more detailed definition see [18]). Let $\boldsymbol{\Phi}(x_1, \ldots, x_n)$ be a joint multivariate distribution function with univariate marginal distribution functions $\Phi_1, \ldots, \Phi_n$, e.g.

$$\Phi_k(x) = \int_{-\infty}^{x} f_k(y)\,\mathrm{d}y,\ k = 1, \ldots, n\,, \tag{2.12}$$

where f_k is the kth respective univariate transition PDF. Then, according to Sklar's theorem there exists a unique copula function $\mathcal{C}(u_1, \ldots, u_n)$ such that

$$\boldsymbol{\Phi}(x_1, \ldots, x_n) = \mathcal{C}(\Phi_1(x_1), \ldots, \Phi_n(x_n)). \tag{2.13}$$

The multivariate joint density function $\mathbf{f}$ is then obtained by differentiating equation (2.13):

$$\mathbf{f}(x_1, \ldots, x_n) = \frac{\partial^n \boldsymbol{\Phi}(x_1, \ldots, x_n)}{\partial x_1 \cdots \partial x_n} = \frac{\partial^n \mathcal{C}(\Phi_1(x_1), \ldots, \Phi_n(x_n))}{\partial \Phi_1(x_1) \cdots \partial \Phi_n(x_n)} f_1(x_1) \cdots f_n(x_n). \tag{2.14}$$

Suppose that $f_k(x)$, $k = 1, \ldots, n$, be given by the transition PDFs of the processes $(X_t^{(\rho_k,k)})_{t\geq 0}$, i.e., $f_k(x) = p_X^{(\rho_k,k)}(t; x_{0,k}, x)$ where $x_{0,k} \equiv X_0^{(\rho_k,k)}$. The univariate marginal distributions are each defined by

$$\Phi^{\rho_k,k}(t; x_{0,k}, x) := \int_{-\infty}^{x} p_X^{(\rho_k,k)}(t; x_{0,k}, y)\,\mathrm{d}y = \mathbb{P}(X_t^{(\rho_k,k)} \leq x \mid x_{0,k})\,,\quad k = 1, \ldots, n. \tag{2.15}$$

Then the joint multivariate CDF of the process $(\mathbf{X}_t^{(\boldsymbol{\rho})})_{t\geq 0}$ started at $\mathbf{x}_0 = (x_{0,1}, \ldots, x_{0,n})$ is given by the copula:

$$\begin{aligned}\boldsymbol{\Phi}^{(\boldsymbol{\rho})}(x_1, \ldots, x_n) &:= \mathbb{P}(X_t^{\rho_1,1} \leq x_1, \ldots, X_t^{\rho_n,n} \leq x_n \mid \mathbf{x}_0) \\ &= \mathcal{C}(\mathbb{P}(X_t^{\rho_1,1} \leq x_1 \mid x_{0,1}), \ldots, \mathbb{P}(X_t^{\rho_n,n} \leq x_n \mid x_{0,n})) \\ &= \mathcal{C}(\Phi^{\rho_1,1}(t; x_{0,1}, x_1), \ldots, \Phi^{\rho_n,n}(t; x_{0,n}, x_n))\,.\end{aligned} \tag{2.16}$$

One important example of copula functions often used for modeling in finance is the Gaussian copula. This copula is constructed from the multivariate normal distribution:

$$\mathcal{C}_R^{Gauss}(u_1, \ldots, u_n) = \mathcal{N}_R\left(\mathcal{N}^{-1}(u_1), \ldots, \mathcal{N}^{-1}(u_n)\right)\,, \tag{2.17}$$

where $\mathcal{N}_R$ is the standard n-variate normal CDF with correlation matrix R (i.e., $R = R^T > 0$, $\forall i, j\, \{R\}_{i,j} \in [-1:1]$ and $\{R\}_{i,i} = 1$) and zero mean vector. $\mathcal{N}^{-1}$ stands for the inverse of a standard univariate normal CDF, i.e.,

$$\mathcal{N}(x) = \frac{1}{\sqrt{2\pi}} \int_{-\infty}^{x} e^{-y^2/2}\, \mathrm{d}y\,.$$

The multivariate density function $\mathbf{f}$ in (2.14) has the following form (using $u_k = \Phi_k(x_k)$, $z_k = \mathcal{N}^{-1}(u_k)$):

$$\begin{aligned}\mathbf{f}(x_1, \ldots, x_n) &= \frac{\partial^n \mathcal{C}_R^{Gauss}(\Phi_1(x_1), \ldots, \Phi_n(x_n))}{\partial u_1 \cdots \partial u_n} f_1(x_1) \cdots f_n(x_n) \\ &= \frac{\partial^n \mathcal{N}_R\left(z_1, \ldots, z_n\right)}{\partial z_1 \cdots \partial z_n} \prod_{k=1}^{N} \frac{\partial \mathcal{N}^{-1}(u_k)}{\partial u_k} f_k(x_k) \\ &= \phi_R\left(\mathcal{N}^{-1}(u_1), \ldots, \mathcal{N}^{-1}(u_n)\right) \prod_{k=1}^{N} \frac{f_k(x_k)}{\phi(\mathcal{N}^{-1}(u_k))} \\ &= \frac{\phi_R\left(\mathcal{N}^{-1}(\Phi_1(x_1)), \ldots, \mathcal{N}^{-1}(\Phi_n(x_n))\right)}{\phi(\mathcal{N}^{-1}(\Phi_1(x_1))) \cdots \phi(\mathcal{N}^{-1}(\Phi_n(x_n)))} f_1(x_1) \cdots f_n(x_n)\,,\end{aligned} \tag{2.18}$$

where ϕ is the PDF of the standard normal distribution and ϕ_R denotes the joint PDF of the n-variate normal distribution with mean vector zero and covariance matrix R:

$$\begin{aligned}\phi(x) &= \frac{e^{-x^2/2}}{\sqrt{2\pi}}, \\ \phi_R(\mathbf{x}) &= \frac{e^{-\mathbf{x}R^{-1}\mathbf{x}^T}}{\sqrt{\det(2\pi R)}}\,,\ \mathbf{x} = (x_1, \ldots, x_n).\end{aligned} \tag{2.19}$$

2.2.3 Sequential Path Construction

Consider the problem of sampling a multivariate process $(\mathbf{S}_t)$ conditionally on $\mathbf{S}_0 = \left(S_0^1, \ldots, S_0^n\right)$. Suppose that the underlying process $(\mathbf{X}_t^{(\boldsymbol{\rho})})$ has a multivariate distribution given by a Gaussian copula (2.17) with the marginal transition PDFs $p_X^{(\rho_k,k)}(t; x_{0,k}, x)$, $k = 1, 2, \ldots, n$. (Recall $f_k(x) = p_X^{(\rho_k,k)}(t; x_{0,k}, x)$ and $\Phi^k(x) = \int_{-\infty}^{x} f_k(y)\mathrm{d}y$.) Then one should apply the following sampling algorithm:

1. Apply the inverse mapping functions to obtain the initial values of the n-dimensional $\mathbf{X}^{(\boldsymbol{\rho})}$-diffusion:
$$x_{0,k} \equiv X_0^{(\rho_k,k)} = \mathsf{X}^k(S_0^k), \quad k = 1, 2, \ldots, n.$$

2. Sample a normal vector $(z_1, \ldots, z_n)$ from the n-variate normal distribution function $\mathcal{N}_R$ with zero mean vector and correlation matrix R.

3. Obtain uniform variates $u_k = \mathcal{N}(z_k)$, $k = 1, \ldots, n$.

4. For each $k = 1, \ldots, n$ obtain $X_t^k = (\Phi^k)^{-1}(u_k)$ by employing numerical inversion of the CDFs
$$u_k = \Phi^k(X_t^k) = \int_{-\infty}^{X_t^k} p_X^{(\rho_k,k)}(t; x_{0,k}, x)\,\mathrm{d}x, \quad k = 1, 2, \ldots, n.$$

2.2.4 Bridge Path Construction

Suppose that the process $(\mathbf{X}_t^{(\boldsymbol{\rho})})$ conditional on given $\mathbf{X}_0^{(\boldsymbol{\rho})}$ is to be sampled at a set of times $0 = t_0 < t_1 < t_2 < \cdots < t_N = T$. One natural way to generate a trajectory is by applying sequential sampling by generating $\mathbf{X}_{t_i}^{(\boldsymbol{\rho})}$ conditional on $\mathbf{X}_{t_{i-1}}^{(\boldsymbol{\rho})}$ for each $i = 1, \ldots, n$. An alternative approach to generate $(\mathbf{X}_t^{(\boldsymbol{\rho})})$ is by the bridge path construction. The bridge density $b_S(t; S) \equiv b_S(t_1, t_2, t; S_1, S_2, S)$ for $S_t = S$, $t_1 < t < t_2$, conditional on $S_{t_1} = S_1$ and

$S_{t_2} = S_2$, is given by (using the measure change in (1.9)):

$$
\begin{aligned}
b_S(t;S) &= \frac{p_S(t-t_1;S_1,S)p_S(t_2-t;S,S_2)}{p_S(t_2-t_1;S_1,S_2)} \\
&= \frac{\nu}{\sigma(S)} \frac{p_X^{(\rho)}(t-t_1;\mathsf{X}(S_1),\mathsf{X}(S))p_X^{(\rho)}(t_2-t;\mathsf{X}(S),\mathsf{X}(S_2))}{p_X^{(\rho)}(t_2-t_1;\mathsf{X}(S_1),\mathsf{X}(S_2))} \\
&= \frac{\nu}{\sigma(S)} \frac{p_X(t-t_1;\mathsf{X}(S_1),\mathsf{X}(S))p_X(t_2-t;\mathsf{X}(S),\mathsf{X}(S_2))}{p_X(t_2-t_1;\mathsf{X}(S_1),\mathsf{X}(S_2))} \equiv \frac{\nu}{\sigma(S)} b_X(t;\mathsf{X}(S)),
\end{aligned}
\tag{2.20}
$$

where $b_X(t;x) \equiv b_X(t_1,t_2,t;x_1,x_2,x)$ is the bridge PDF of the underlying X-diffusion conditional on the endpoint path values $x_1 = X_{t_1} = \mathsf{X}(S_1)$ and $x_2 = X_{t_2} = \mathsf{X}(S_2)$. As was shown in [12] the bridge PDF b_X of the Ornstein–Uhlenbeck diffusion is a normal density with mean a and variance b^2 given by

$$
\begin{aligned}
a &= \frac{x_1 e^{\lambda\Delta_1}(e^{2\lambda\Delta_2}-1) + x_2 e^{\lambda\Delta_2}(e^{2\lambda\Delta_1}-1)}{e^{2\lambda(\Delta_1+\Delta_2)}-1}, \\
b^2 &= \frac{(e^{2\lambda\Delta_1}-1)(e^{2\lambda\Delta_2}-1)}{\kappa(e^{2\lambda(\Delta_1+\Delta_2)}-1)},
\end{aligned}
\tag{2.21}
$$

where $\Delta_1 \equiv t - t_1$, $\Delta_2 \equiv t_2 - t$, and $\Delta_1 + \Delta_2 = t_2 - t_1$. A construction of the sequence of time points in a bridge algorithm is depicted on Figure 2.2.

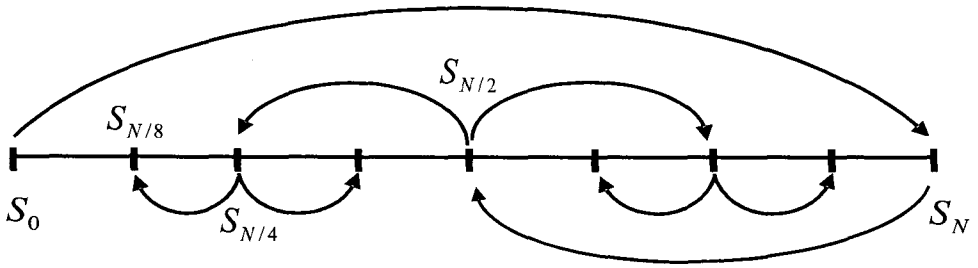

Figure 2.2: Bridge sampling.

2.2.5 Path Sampling with a Bridge Normal Copula

Let $b_X^k(t;x)$ be a bridge PDF conditional on endpoint values $X_0^{(\rho_k,k)}$ and $X_{t_N}^{(\rho_k,k)}$, then b_X^k is a normal density function with mean a_k and variance b_k^2, with values given by (2.21) where $\lambda = \lambda_k$, $\kappa = \kappa_k$, $\Delta_1 = t - t_0$, and $\Delta_2 = t_N - t$. Thus each marginal CDF $\Phi_k(x)$ is a normal

CDF $\mathcal{N}\left(\frac{x-a_k}{b_k}\right)$, which allows us to obtain the multivariate CDF $\mathbf{\Phi} = \mathbf{\Phi}(x_1, \ldots, x_n) = \mathcal{N}_R\left(\frac{x_1-a_1}{b_1}, \cdots, \frac{x_n-a_n}{b_n}\right)$ that corresponds to a multivariate normal distribution with mean vector $(a_1, \ldots, a_n)^\top$ and covariance matrix DRD, where $D = \text{diag}(b_1, \ldots, b_n)$. To sample the multivariate process $(\mathbf{X}_t^{(\boldsymbol{\rho})})$ conditionally on endpoints values $\mathbf{X}_0^{(\boldsymbol{\rho})}$ and $\mathbf{X}_{t_N}^{(\boldsymbol{\rho})}$ for time $t, 0 < t < t_N$, we apply the following algorithm:

1. Sample a normal vector $(z_1, \ldots, z_n)$ from $\mathcal{N}_R$.

2. For each $k = 1, \ldots, n$, set $X_t^k = a_k + b_k z_k$

To obtain the vector of values of the multivariate asset price process $(\mathbf{S}_t)$, map the resulting values of $(\mathbf{X}_t^{(\boldsymbol{\rho})})$:

$$X_t^k \longmapsto S_t^k = \mathsf{F}^k(X_t^k),\ k = 1, 2, \ldots, n.$$

Applying the same technique recursively, one can sample all values of the asset price process $(\mathbf{S}_t)$ between t_0 and t_N.

The exact bridge simulation method provides a powerful tool to improve the effectiveness of quasi-Monte Carlo (QMC) methods by reducing the effective dimension of the problem. The idea is that the first few random numbers that are generated have larger impact on the trajectory under this technique than with the sequential sampling.

2.3 Calibration of the UOU Model to Market Data

2.3.1 Univariate Case

It is very important from the practical point of view to develop a reliable and reasonably quick calibration scheme for the UOU diffusion family. Our objective is to obtain a calibration scheme that provides two levels of calibration: first, an initial full calibration of all parameters of the model and, second, a much faster recalibration that can be used as soon as new data have arrived. The second calibration scheme may be used throughout daily

trading or even for longer periods, while the full calibration only needs to be executed if markets move considerably.

Non-linear Least Squares

To estimate a best-fitted parameter set $\xi = \{\lambda, \nu, a_0, \rho\}$ of the UOU model based on (observed) market option price data, the least squares method is employed. Suppose that a standard call option with strike K_i and maturity T_i has an observed price O_i, while the model produces a price of $C_i = C(K_i, T_i; \xi)$ for the same option, where $i = 1, 2, \ldots, N$. The goal of the calibration process is to minimize the least squares error for the N options considered:

$$F(\xi) = \sum_{i=1}^{N} w_i \left| C(K_i, T_i; \xi) - O_i \right|^2 \to \min_{\xi}, \tag{2.22}$$

where w_i is a weight that reflects the relative importance of reproducing the ith option price precisely.

The suitable choice of the weight factors w_i, $i = 1, 2, \ldots, N$, is crucial for good calibration results. The confidence in individual data points is determined by the liquidity of the option. The weights can be evaluated from the bid-ask spreads: $w_i = |O_i^{\text{ask}} - O_i^{\text{bid}}|^{-1}$. Alternatively, as it was suggested by [7], we use the Black-Scholes (BS) "Vegas" evaluated at the implied volatilities of the market option prices to compute the weights: $w_i = \left(\partial C^{\text{BS}}(\sigma_i^{\text{BS}})/\partial\sigma\right)^{-2}$, where $\partial C^{\text{BS}}/\partial\sigma$ denotes the derivative of the BS option pricing formula with respect to the volatility σ, and $\sigma_i^{\text{BS}} = \sigma^{\text{BS}}(O_i, K_i, T_i)$ is the BS implied volatility for the observed market price O_i.

Regularization

In general, the calibration of a pricing model is an inverse problem, whose solution depends discontinuously on the data. To achieve uniqueness and stability of the solution, a penalty

function is added to the least squares term:

$$F_\alpha(\xi) = \sum_{i=1}^{N} w_i \left| C(K_i, T_i; \xi) - O_i \right|^2 + \alpha H(\mathbb{P}, \mathbb{P}_0) \to \min_{\xi}, \tag{2.23}$$

where the penalty function H is chosen such that the problem becomes well-posed.

As is examined in [7], the relative entropy method may be applied for solving ill-posed calibration problems. The relative entropy of a probability measure $\mathbb{P}$ on sample space Ω with respect to some primal measure $\mathbb{P}_0$ is defined as follows:

$$\begin{aligned} H(\mathbb{P}, \mathbb{P}_0) &= \mathbb{E}^{\mathbb{P}} \left[\ln \frac{\mathrm{d}\mathbb{P}}{\mathrm{d}\mathbb{P}_0} \right] = \int_{\Omega} \ln \frac{\mathrm{d}\mathbb{P}}{\mathrm{d}\mathbb{P}_0} \, \mathrm{d}\mathbb{P} \\ &= \int_0^{\infty} \ln \left(\frac{p_S(T; S_0, S; \xi)}{p_S(T; S_0, S; \xi_0)} \right) p_S(T; S_0, S; \xi) \, \mathrm{d}S, \end{aligned} \tag{2.24}$$

where $T = 1$ corresponds to 1 year time interval.

The regularization parameter α in (2.23) is used to adjust the trade-off between the accuracy of calibration and the numerical stability of results with respect to the input option data. The right choice of α is based on the Morozov discrepancy principle [19], which is described by the following algorithm:

1. Compute parameters of ξ_0 of the primal measure $\mathbb{P}_0$ by solving the nonlinear least squares problem (2.22) in low precision. Alternatively, one may compute ξ_0 by fitting the model to historical asset price returns.

2. Fix $\delta \in (1, 1.5)$ and numerically solve equation $F_\alpha(\xi_0) = \delta F(\xi_0)$ for the regularization parameter α, where $F_\alpha(\xi_0)$ is defined in (2.23).

2.3.2 Numerical Results for the Univariate Case

The data set used consists of 79 European call option prices with maturities ranging from less than one month up to 1.56 years. These market prices were obtained from Yahoo for IBM having the spot share value of 101.34 on July 7th, 2009. For the sake of simplicity, the risk-free interest is assumed to be constant and equal to $r = 0.25\%$, and the dividend

rate is set to zero. The calibration routine was developed using Matlab with Optimization Toolbox, running on an Intel Core 2 CPU 2.14GHz with 2 GB of main memory.

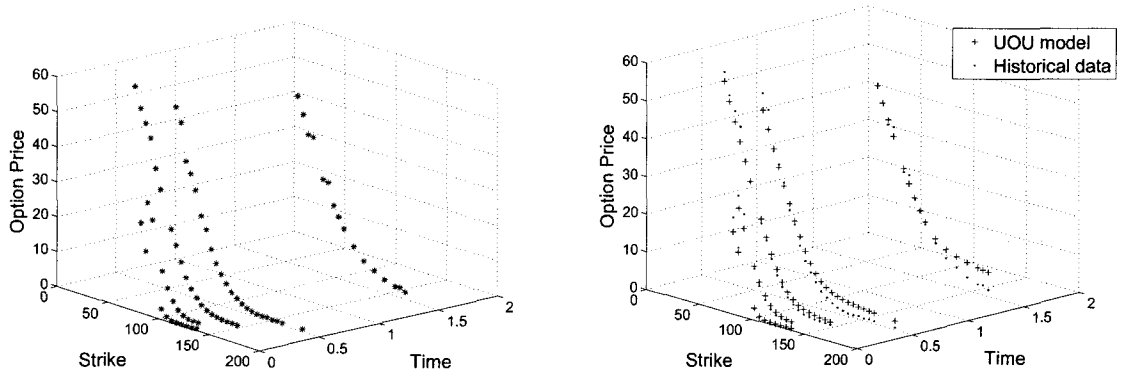

Figure 2.3: Market option call price surface for IBM, July 7th, 2009 (left plot). Comparison of quoted option mid prices and option prices calculated using the UOU model with the optimal parameter set (right plot).

To obtain the set of parameters for the primal probability measure, the UOU model is calibrated to the historical data from May 7th to July 7th, 2009. Using historical asset prices, $\widehat{S}_{t_j}$, $j = 0, 1, \ldots, N$, $0 = t_0 < t_1 < \cdots < t_N$, and the transition densities, we obtain the following (single-asset) log-likelihood function for this set of observations:

$$\begin{aligned} L_1(\xi) &= \sum_{j=1}^{N} \ln p_S(t_j - t_{j-1}; \widehat{S}_{t_{j-1}}, \widehat{S}_{t_j}; \xi) \\ &= \sum_{j=1}^{N} \ln \left(\frac{\nu}{\sigma(\widehat{S}_{t_j}; \xi)} p_X^{(\rho)} \left(t_j - t_{j-1}; \mathsf{X}(\widehat{S}_{t_{j-1}}; \xi), \mathsf{X}(\widehat{S}_{t_j}; \xi); \xi \right) \right). \end{aligned} \tag{2.25}$$

Here, we assume the sequential simulation method.

In practice, the implementation of the calibration procedure is started with some initial values of model parameters. The upper and lower bounds for the parameters should also be provided. Based on empirical analysis, such bounds are obtained and are provided in Table 2.1.

Parameter	ρ	υ	a_0	κ
Lower bound	0.001	0.005	45	0.5
Upper bound	0.5	2	250	10
Initial value	0.04	0.34	102.59	1

Table 2.1: Initial values and bounds for the parameters of the UOU model.

Running on an Intel Core 2 CPU 2.14GHz with 2 GB of main memory, the calibration procedure takes approximately 200 seconds to fit the model to 63 historical asset prices. The optimal values, that maximize the log-likelihood function (2.25), are $\rho = 0.0357$, $\upsilon = 0.0531$, $a_0 = 118.2404$, $\kappa = 0.5951$. This set of parameters defines the primal probability measure. The estimation of the regularization parameter α in formula (2.23) is based on the algorithm described above. The calculated value of α is 0.266.

The final step of the calibration process is the minimization of the nonlinear least squares function regularized by the relative entropy as is given in (2.23). The computation algorithm utilizes the Matlab function lsqnonlin with the exit tolerance set to 10^{-6}. This function employs the Levenberg-Marquardt least-squares algorithm for estimating optimal parameters. The starting values and the limits for the parameters remain the same as given in Table 2.1. The computational time is approximately 400 seconds to fit the model to 79 option prices. The best-fitted parameters of the model are $\rho = 0.0203$, $\upsilon = 0.0013$, $a_0 = 102.1384$, $\kappa = 0.6579$. The objective function F_α attains its minimum value of 1.58.

The discrepancy between the computed option prices and observed option prices may originate from different sources. First, the market data may contain errors or misleading information. For example, the values of illiquid options might be mispriced, or simple input errors may occur. Second, the calibration procedure estimates model parameters of an arbitrage-free model, while the market prices are not necessarily arbitrage-free. Hence, there is an inherent mismatch between the model prices and the market data. Notice that the use of time-dependent parameters may decrease the level and number of errors and

make the calibration procedure maturity-wise. Another possible solution to improve the accuracy is to employ the calibration separately for out-of-the-money, at-the-money and in-the-money options. Of course, a source of error that will always exist with any model is the specification of the model itself.

2.3.3 Multivariate Case

Let us consider the multi-asset price processes $(\mathbf{S}_t)_{t\geq 0}$ that follows a multivariate UOU model, where univariate UOU diffusions are coupled via the Gaussian copula function.

The calibration procedure can be split into two stages:

1. Estimation of the parameters of the marginal (single-asset price) processes.
2. Estimation of the correlation matrix R of the Gaussian copula.

Such a calibration algorithm admits multiple variations. First, one may use maximum likelihood estimation (MLE) to fit the marginal models to historical asset prices. Second, one may use the least squares method to fit the marginal models to historical derivative prices (say European options). For both approaches, the correlation matrix is then estimated by MLE using historical asset prices. Alternatively, one may use only observed asset prices to estimate all parameter of the multivariate model simultaneously without splitting the calibration process. However, in this case the computation time will increase significantly due to higher dimensionality of the optimization problem. Notice also that the multivariate path distribution depends on the simulation method used. By using the sequential sampling or some version of the bridge sampling, one may obtain different models and, hence, obtain slightly different estimates of the model parameters.

Let $\left\{(\widehat{S}^1_{t_j},\ldots,\widehat{S}^n_{t_j})\right\}_{j=0}^{N}$ be the $n\times(N+1)$ matrix containing $N+1$ independent historical prices for each of the n financial assets observed on a set of time points $\mathbf{T}=\{t_0,t_1,\ldots,t_N\}$. Let $(\boldsymbol{\xi},R)=(\xi_1,\ldots,\xi_n,R)$ denote the set of model parameters to be estimated. The historical observations in $X^{(\rho)}$-space are obtained by applying the inverse map $\widehat{X}^k_{t_j}=\mathsf{X}^k(\widehat{S}^k_{t_j})$.

Assume that $\widetilde{\mathbf{T}} = \{\tilde{t}_j\}_{j=0}^N$ represent some arrangement of time points in $\mathbf{T}$. The ordering of the time points is determined by the simulation method used. For the (forward) sequential method we assume that $0 = \tilde{t}_0 < \tilde{t}_1 < \cdots < \tilde{t}_N = T$, i.e., $\forall j \geq 0\ \tilde{t}_j = t_j$. For the backward-in-time bridge method we have that $0 = \tilde{t}_0 < \tilde{t}_N < \tilde{t}_{N-1} < \cdots < \tilde{t}_2 < \tilde{t}_1 = T$, i.e., $\forall j \geq 1\ \tilde{t}_j = t_{N+1-j}$.

Let $f_j^k(x)$ denote the PDF of $X_{\tilde{t}_j}^{(\rho_k,k)}$ conditional on the σ-algebra $\mathcal{F}_{j-1}^k$ generated by the first j sample path points $X_0^{(\rho_k,k)}, X_{\tilde{t}_1}^{(\rho_k,k)}, \ldots, X_{\tilde{t}_{j-1}}^{(\rho_k,k)}$, where $1 \leq j \leq N$ and $1 \leq k \leq n$. For the sequential path sampling method, with $\tilde{t}_i = t_i$, we have that $f_j^k(x) = p_X^{(\rho_k,k)}\left(t_j - t_{j-1}; X_{t_{j-1}}^{(\rho_k,k)}, x\right)$. For the backward bridge method we have that $f_j^k(x) = b_X^k\left(\tilde{t}_j; x\right)$ is a bridge PDF of the Ornstein–Uhlenbeck bridge conditional on $X_0^{(\rho_k,k)}$ and $X_{\tilde{t}_{j-1}}^{(\rho_k,k)}$, where $\tilde{t}_j = t_{N+1-j}$ and $\tilde{t}_{j-1} = t_{N+2-j}$. Let Φ_j^k denote the CDF that corresponds to the PDF f_j^k.

Suppose the joint transition PDF of the process $(\mathbf{X}_t^{(\rho)})$ is constructed with the Gaussian copula as given by (2.13) and (2.17). The n-asset log-likelihood function is then

$$\begin{aligned} L_n(\boldsymbol{\xi}, R) = &\sum_{j=1}^{N} \ln\left(\frac{\phi_R(\mathcal{N}^{-1}(\Phi_j^1(\widehat{X}_{\tilde{t}_j}^1;\xi_1)),\ldots,\mathcal{N}^{-1}(\Phi_j^n(\widehat{X}_{\tilde{t}_j}^n;\xi_n)))}{\phi(\mathcal{N}^{-1}(\Phi_j^1(\widehat{X}_{\tilde{t}_j}^1;\xi_1)))\cdots\phi(\mathcal{N}^{-1}(\Phi_j^n(\widehat{X}_{\tilde{t}_j}^n;\xi_n)))}\right) \\ &+ \sum_{k=1}^{n}\sum_{j=1}^{N} \ln\left(\frac{\nu_k}{\sigma^k(\widehat{S}_{\tilde{t}_j}^k)} f_j^k(\widehat{X}_{\tilde{t}_j}^k;\xi_k)\right) \equiv L_n^{\text{corr}}(R|\boldsymbol{\xi}) + \sum_{k=1}^{n} L_1(\xi_k), \end{aligned} \tag{2.26}$$

where ϕ_R denotes the joint PDF of the n-variate normal distribution with mean vector zero and covariance matrix R; L_1 is the single-asset log-likelihood function given by (2.25), and L_n^{corr} denotes the log-likelihood function for the copula function. Recall that the expression in (2.26) is independent of the simulation method used. For the sequential and bridge methods, we provide below specific expressions of the log-likelihood function.

As is suggested by the structure of the log-likelihood function in (2.26), the calibration process can be split into two steps. First, the sets $\xi_k = \{\lambda_k, \nu_k, a_{0k}, \rho_k\}$, $k = 1, 2, \ldots, n$ of parameters of the marginal distributions are estimated by employing maximum likelihood

estimation:

$$\widehat{\xi}_k = \arg\max_{\xi_k} L_1(\xi_k) = \arg\max_{\xi_k} \sum_{j=1}^{N} \ln\left(\frac{\nu_k}{\sigma^k(\widehat{S}^k_{t_j})} f_j^k(\widehat{X}^k_{t_j};\xi_k)\right), \quad k=1,\ldots,n. \tag{2.27}$$

As is seen, the parameters of the marginal distributions are estimated based on historical data. An alternative approach to computing the parameters is to fit asset price distributions to observed option prices.

The last step is to estimate the correlation matrix R for the given optimal model parameters $\widehat{\boldsymbol{\xi}} \equiv \{\widehat{\xi}_1,\ldots,\widehat{\xi}_n\}$ estimated from the previous step.

Sequential calibration.

For the sequential path generation method, the algorithm is as follows.

(i) Map all the observations into $X^{(\rho)}$-space using the respective inverse maps:

$$\mathbf{X}_j \equiv (\widehat{X}^1_j,\ldots,\widehat{X}^n_j) = ((\mathsf{X}^1(\widehat{S}^1_{t_j};\hat{\xi}^1),\ldots,\mathsf{X}^n(\widehat{S}^n_{t_j};\hat{\xi}^n)), \quad j=0,\ldots,N.$$

(ii) Compute vectors $\mathbf{u}_j \equiv (u_j^1,\ldots,u_j^n) \in [0,1]^n$, by evaluating the integrals:

$$u_j^k = \int_{-\infty}^{\widehat{X}^k_j} p_X^{(\rho_k,k)}(t_i - t_{j-1};\widehat{X}^k_{j-1},x;\widehat{\xi}_k)\,\mathrm{d}x, \quad j=1,\ldots,N$$

(iii) Maximize the log-likelihood function with respect to R:

$$\sum_{j=1}^{N} \ln\phi_R\left(\mathcal{N}^{-1}(u_j^1),\ldots,\mathcal{N}^{-1}(u_j^n)\right) \to \max_R.$$

Bridge calibration.

The estimation of the log-likelihood function for the sequential calibration involves numerous estimations of the CDF for the UOU model. Since there is no simple-form solution for

the CDF, the numerical integration of the probability density function should be performed regularly. By applying the bridge approach to the construction of the multivariate path distribution function, the number of integrals to be computed numerically on step (ii) reduces from $n \times N$ to n. This is due to the fact that for the bridge approach, the marginal CDFs Φ_j^k, $j = 2, \ldots, N$, are Gaussian. Hence, for the backward-in-time bridge path generation method, the log-likelihood function can be simplified as follows:

$$L_n^{\text{corr}}(R|\hat{\boldsymbol{\xi}}) = \sum_{j=2}^{N} \ln \left(\frac{\phi_R(x_j^1, \ldots, x_j^n)}{\phi(x_j^1) \cdots \phi(x_j^n)} \right) + \ln \left(\frac{\phi_R(\mathcal{N}^{-1}(\Phi_1^1(\widehat{X}_{\tilde{t}_1}^1; \xi_1)), \ldots, \mathcal{N}^{-1}(\Phi_1^n(\widehat{X}_{\tilde{t}_1}^n; \xi_n)))}{\phi(\mathcal{N}^{-1}(\Phi_1^1(\widehat{X}_{\tilde{t}_1}^1; \xi_1))) \cdots \phi(\mathcal{N}^{-1}(\Phi_1^n(\widehat{X}_{\tilde{t}_1}^n; \xi_n)))} \right), \tag{2.28}$$

where $x_j^k = \dfrac{\widehat{X}_{\tilde{t}_j}^k - a_{kj}}{b_{kj}}$; mean a_{kj} and variance b_{kj}^2 are computed by formulae in (2.21) using $\lambda = \lambda_k, \kappa = \kappa_k, \Delta_1 = \tilde{t}_j - \tilde{t}_{j-1}, \Delta_2 = \tilde{t}_{j+1} - \tilde{t}_j$.

The following algorithm can be applied for the backward-in-time bridge path generation method.

(i) Map the observations into $X^{(\rho)}$-space $\mathbf{S}_j \to \mathbf{X}_j = \mathsf{F}^{-1}(\mathbf{S}_j; \hat{\boldsymbol{\xi}}), j = 1, \ldots, N$, as is described in part (i) of the sequential algorithm.

(ii) For each $k = 1, \ldots, n$ and $j = 1, \ldots, N-1$ calculate a_{kj} and b_{kj} by using (2.21) with respective parameters $\lambda = \lambda_k$, $\kappa = \kappa_k$, $\Delta_1 = t_j - t_{j-1}$, and $\Delta_2 = t_{j+1} - t_j$. Then, set

$$x_j^k = \frac{\widehat{X}_j^k - a_{kj}}{b_{kj}}.$$

(iii) Compute $\mathbf{u}_N \equiv (u_N^1, \ldots, u_N^n)$, the values of normal CDFs corresponding to the terminal point of a path:

$$u_N^k = \int_{-\infty}^{\widehat{X}_N^k} p_X^{(\rho_k, k)}(t_N - t_{N-1}; \widehat{X}_{N-1}^k, x; \widehat{\xi}_k)\, \mathrm{d}x, \quad k = 1, \ldots, n. \tag{2.29}$$

(iv) Maximize the log-likelihood function with respect to R:

$$\sum_{j=1}^{N-1} \ln \phi_R\left(x_j^1, \ldots, x_j^n\right) + \ln \phi_R\left(\mathcal{N}^{-1}(u_N^1), \ldots, \mathcal{N}^{-1}(u_N^n)\right) \to \max_R.$$

Numerical Results for the Multivariate Case

For this numerical experiment the daily observations of four American companies, namely, IBM, Microsoft, Pepsi, and Walmart, have been collected from YAHOO!^{TM}. The examined period is April 7th, 2009, to July 7th, 2009, and it consists of 63 time points. In the first stage of the calibration, the optimal sets of parameters of the marginal distributions are estimated by solving equation (2.27), and they are provided in Table 2.2.

	IBM	Microsoft	Pepsi	Walmart
ρ	0.0496	0.2173	0.0865	0.0493
υ	0.0887	0.0365	0.1149	0.0886
a_0	103.9904	21.1638	31.671	52.3842
κ	0.9670	0.874	0.910	0.9874

Table 2.2: Optimal parameters estimated for IBM, Microsoft, Pepsi, and Walmart

Two approaches are then used for the evaluation of the optimal correlation matrix R. In the first approach, the correlation matrix is obtained by the pairwise calculation of the correlation coefficients. There are $\binom{4}{2}$ correlation coefficients for 4 stock-price processes to be calculated. However, the resulting matrix may violate the positive-definite property of a correlation matrix. To overcome this problem, a method suggested by [20] of finding the closest correlation matrix by the spectral decomposition is applied.

The idea of the spectral decomposition method is to obtain a valid $(N \times N)$ correlation matrix $\widetilde{C}$ that best fits a given, not necessarily positive-definite $N \times N$ matrix C. Given the eigensystem S and associated set of eigenvalues $\{\lambda_i\}$, a real symmetric matrix C can be written as

$$C = S\Lambda S^T, \quad \text{where } \Lambda = \text{diag}(\lambda_1, \ldots, \lambda_N)\,.$$

If the matrix C is not positive-definite, it has at least one negative eigenvalue. By setting the negative eigenvalues to small positive number ϵ, we define the elements of the diagonal

matrix $\Lambda' = \mathrm{diag}(\lambda'_1, \ldots, \lambda'_N)$ as

$$\lambda'_i = \begin{cases} \lambda_i, & \lambda_i \geq 0, \\ \epsilon, & \lambda_i < 0, \end{cases} \quad i = 1, \ldots, N.$$

To obtain unit diagonal correlation elements we set the non-zero elements of the diagonal scaling matrix $L = \mathrm{diag}(l_1, \ldots, l_N)$ with respect to the eigensystem S by

$$l_i = \left(\sum_{j=1}^{N} s_{ij}^2 \lambda'_j \right)^{-1}, \quad i = 1, \ldots, N.$$

Then, one can obtain a positive-definite matrix with unit diagonal elements as

$$\tilde{C} = \sqrt{L} S \Lambda' S^T \sqrt{L}.$$

The results of the numerical experiment are shown in Figure 2.4. The computation time for the bridge simulation is 1.5 times faster than for the sequential simulation.

$$\begin{pmatrix} 1 & 0.297 & 0.151 & 0.337 \\ 0.297 & 1 & 0.089 & -0.045 \\ 0.151 & 0.089 & 1 & -0.080 \\ 0.337 & -0.045 & -0.080 & 1 \end{pmatrix} \qquad \begin{pmatrix} 1 & 0.278 & 0.243 & 0.336 \\ 0.278 & 1 & 0.184 & -0.050 \\ 0.243 & 0.184 & 1 & -0.051 \\ 0.336 & -0.050 & -0.051 & 1 \end{pmatrix}$$

Figure 2.4: Correlation matrices obtained by using the bridge path simulation (left matrix) and the sequential path simulation (right matrix). The pairwise computation of the correlation coefficients is employed.

In the second method, the correlation matrix as a whole is estimated. The computation of an optimal correlation matrix is performed in Matlab using the function fmincon, which allows us to find a minimum of a multivariate function with non-linear constraints. By adding nonlinear constraints, the algorithm works in the class of semi-positive matrices, which is absolutely necessary for the correct formulation of the correlation matrix. However, the candidate matrix, which minimizes the objective function in (2.26), may not have ones on the principal diagonal. To obtain a correct correlation matrix that is closest to the

given one, the spectral decomposition method is applied again. The results are shown in Figure 2.5 and Figure 2.6.

$$\begin{pmatrix} 1.000 & 0.277 & 0.169 & 0.335 \\ 0.277 & 0.993 & 0.127 & -0.049 \\ 0.169 & 0.127 & 0.480 & -0.024 \\ 0.335 & -0.049 & -0.024 & 0.993 \end{pmatrix} \xrightarrow[\text{decomp.}]{\text{spect.}} \begin{pmatrix} 1 & 0.278 & 0.243 & 0.336 \\ 0.278 & 1 & 0.183 & -0.049 \\ 0.243 & 0.183 & 1 & -0.035 \\ 0.336 & -0.049 & -0.035 & 1 \end{pmatrix}$$

Figure 2.5: The candidate semi-positive matrix that minimizes the objective function (2.26) (left matrix) obtained by using the sequential simulation method and the closest correlation matrix obtained by using the spectral decomposition method (right matrix).

$$\begin{pmatrix} 1.000 & 0.290 & 0.145 & 0.335 \\ 0.290 & 0.973 & 0.084 & -0.043 \\ 0.145 & 0.084 & 0.966 & -0.076 \\ 0.335 & -0.043 & -0.076 & 0.993 \end{pmatrix} \xrightarrow[\text{decomp.}]{\text{spect.}} \begin{pmatrix} 1 & 0.293 & 0.148 & 0.336 \\ 0.293 & 1 & 0.086 & -0.043 \\ 0.148 & 0.086 & 1 & -0.078 \\ 0.336 & -0.043 & -0.078 & 1 \end{pmatrix}$$

Figure 2.6: The candidate semi-positive matrix that minimizes the objective function (2.26) (left matrix) obtained by using the bridge simulation method and the closest correlation matrix obtained by using the spectral decomposition method (right matrix).

3 Credit Risk Modeling with the Confluent–U Model

3.1 The Family of Confluent Hypergeometric Models

We now consider a diffusion process $(S_t)_{t\geq 0}$ of the form (1.1), in which the underlying X-diffusion is a Cox-Ingerssol-Ross (CIR) process $(X_t)_{t\geq 0} \in \mathcal{I} = (0,\infty)$ with SDE [21]

$$dX_t = (\alpha_0 - \alpha_1 X_t)dt + \nu\sqrt{X_t}dW_t, \quad t > 0, \tag{3.1}$$

where α_0, α_1, ν are positive constants, and $(W_t)_{t\geq 0}$ is a standard Brownian motion. With the condition $\mu := \frac{2\alpha_0}{\nu^2} - 1 > 0$ the process $(X_t)_{t\geq 0}$ is conservative on $\mathcal{I}$ (the origin is entrance and ∞ is a non-attracting natural boundary). The speed and scale densities are

$$\mathfrak{s}(x) = x^{-\mu-1}e^{\kappa x}, \quad \mathfrak{m}(x) = \frac{2}{\nu^2}x^{\mu}e^{-\kappa x}, \tag{3.2}$$

where $\kappa := \frac{2\alpha_1}{\nu^2}$. The transition PDF of the CIR process on $(0,\infty)$ is given by

$$p_X(t; x_0, x) = c_t e^{\alpha_1 t}\left(\frac{xe^{\alpha_1 t}}{x_0}\right)e^{-c_t(xe^{\alpha_1 t}+x_0)}I_\mu(2c_t\sqrt{xx_0e^{\alpha_1 t}}), \tag{3.3}$$

where $c_t := \kappa/(e^{\alpha_1 t} - 1)$ and $I_\mu(x)$ is the modified Bessel function of the first kind.

Applying the diffusion canonical transformation methodology described in Section 1.1 with the choice of coefficients $q_2 = 1, q_1 = 0, c_2 = 0, c_1 = a_0$ leads to the Confluent–U model with generating function

$$\hat{u}_\rho(x) = \mathcal{U}(v, \mu+1, \kappa x), \tag{3.4}$$

where $v := \rho/\alpha_1 > 0$, ρ is an arbitrary positive constant, and $\mathcal{U}(a,b,z)$ is the confluent hypergeometric function of the second kind or Tricomi function, see [17] for details. A pair of fundamental solutions (for any $\rho > 0$) in this case are:

$$\varphi_\rho^+(x) = \mathcal{M}(v, \mu+1, \kappa x)\,, \quad \varphi_\rho^-(x) = \mathcal{U}(v, \mu+1, \kappa x)\,,$$

where $\mathcal{M}(a,b,z)$ is the confluent hypergeometric function of the first kind or Kummer's function, see [17]. Then according to equation (1.10) the mapping function is

$$\mathsf{F}(x) = a_0 \frac{\mathcal{M}(v+\frac{r}{\alpha_1}, \mu+1, \kappa x)}{\mathcal{U}(v, \mu+1, \kappa x)}, \tag{3.5}$$

and it has unique inverse $\mathsf{X} = \mathsf{F}^{-1}$. This construction leads to S-diffusions with diffusion coefficient (1.12) of the form [14]

$$\begin{aligned}\sigma(S) = \nu|\mathsf{F}'(x)| = a_0\kappa\nu\sqrt{x}\Bigg[&\frac{v\mathcal{M}(v+\frac{r}{\alpha_1}, \mu+1, \kappa x)\mathcal{U}(v+1, \mu+2, \kappa x)}{\mathcal{U}^2(v, \mu+1, \kappa x)} \\ &+ \frac{(v+\frac{r}{\alpha_1})\mathcal{M}(v+\frac{r}{\alpha_1}+1, \mu+2, \kappa x)}{(\mu+1)\mathcal{U}(v, \mu+1, \kappa x)}\Bigg], \quad \text{where } x = \mathsf{X}(S).\end{aligned} \tag{3.6}$$

The volatility function $\sigma(S)$ depends on a set of several adjustable positive parameters $\xi = \{a_0, \mu, \alpha_1, \rho, \nu\}$ and drift rate r. It is worth noting that for the driftless case, with $r = 0$, the formula (3.6) reduces to

$$\sigma(S) = \frac{a_0\nu w_\rho e^{\kappa x}}{x^{\mu+1/2}\,\mathcal{U}^2(v, \mu+1, \kappa x)}, \tag{3.7}$$

where $w_\rho = (\Gamma(\mu+1)/\Gamma(v))\,\kappa^{-\mu}$ is a Wronskian constant. As is seen in Figure 3.1, typical plots of the local volatility function $\sigma(S)/S$ generated by formula (3.6) have a pronounced smile-like pattern.

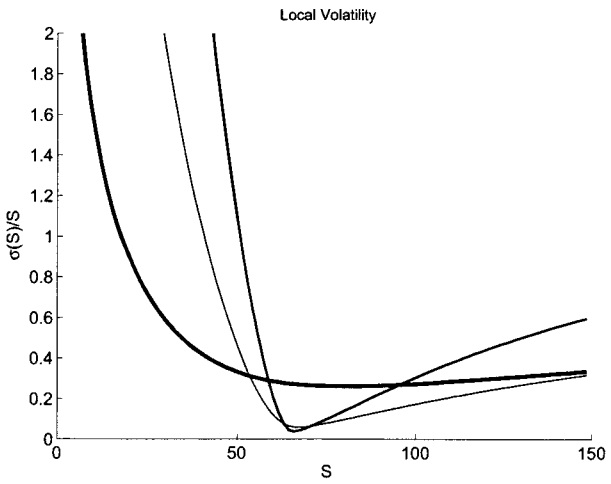

Figure 3.1: Local volatility function $\sigma(S)/S$ for the Confluent–U model. The curves are plotted using the model parameters $\xi = \{65, 1.25, 0.1, 0.001, 2, 0.02\}$ (the thinnest line), $\xi = \{65, 1.25, 0.1, 0.02, 2, 0.02\}$ (the moderate line), $\xi = \{65, 1.25, 0.25, 0.001, 2, 0.02\}$ (the thickest line).

As is shown in [11] the discounted Confluent–U process $(e^{-rt}S_t)_{t\geq 0}$ is a martingale under the assumed risk-neutral measure which we shall denote by $\mathbb{P}$. The transition density of the regular Confluent–U process on $(0, \infty)$ by substituting (3.3), (3.4), (3.6) into (1.9) has the following representation:

$$p_S(t; S_0, S) = \frac{\nu\sqrt{x}e^{-\rho t}}{\sigma(S)} \frac{\mathcal{U}(v, \mu+1, \kappa x)}{\mathcal{U}(v, \mu+1, \kappa x_0)} p_X(t; x_0, x) = \frac{\nu\sqrt{x}}{\sigma(S)} p_X^{(\rho)}(t; x_0, x), \tag{3.8}$$

where $x = \mathsf{X}(F), x_0 = \mathsf{X}(F_0)$. The lower endpoint $\mathsf{F}(0+) = 0$ is an *absorbing boundary* and the upper endpoint $\mathsf{F}(\infty) = \infty$ is a *non-attracting natural boundary* for the S-diffusion with diffusion coefficient in (3.6) and SDE (1.1).

3.2 The Confluent–U Default Model

There exist two main approaches in credit risk modeling: structural models and reduced form models. The structural, or firm based, credit default model, originated from the work of Black and Scholes (1973) in [22] and Merton (1974) in [23]. Such structural models assume that a firm would default if its asset value falls below a certain default level. The

general problem with asset value models is that asset value processes are not observable.

In contrast to structural models, reduced-form credit models use market prices of defaultable instruments (such as bonds or credit default swaps) to extract firm's default probabilities. Initiated by Jarrow/Turnbull (1995) [24], in a reduced-form model, default is treated as an exogenous event. The main weakness of reduced form models is that they do not make effective use of balance sheet and stock market information.

The approach developed in this chapter exploits some of the benefits of structural models in conjunction with reduced-form models. In particular, we put forth an *equity-based structural model of default.* The model allows us to link the pricing of equity options to the pricing of defaultable bonds on a given firm. Our model shares similarities with recent works by Linetsky [25], Carr and Linetsky [26]. However, rather than using a jump to default process, our model is based on the first hitting time of the equity price which is assumed to follow a diffusion with nonlinear (smile-like) volatility.

Let the equity price (i.e., stock share) of a company be described by a stochastic process $(S_t)_{t\geq 0}$ with currently observed price S_0. According to the simplest case of a first passage time methodology, the default event occurs at the first time τ_{def} at which the stock price falls below some default trigger (barrier) level $B \geq 0$, where $S_0 \geq B$:

$$\tau_{def} \equiv \tau_B := \inf\{t \geq 0 : S_t \leq B\}. \tag{3.9}$$

In this thesis we deal with diffusions whose sample paths are continuous functions of time, and hence the first passage time is a first hitting time for the process, i.e.,

$$\tau_{def} \equiv \tau_B := \inf\{t \geq 0 : S_t = B\}. \tag{3.10}$$

Assume that the firm's equity price process $(S_t)_{t\geq 0}$ belongs to the Confluent–U family defined in Section 3.1 with the set of parameters $\xi = \{a_0, \mu, \alpha_1, \rho, \nu\}$. For $S_0 \geq B$ the probability of default $P_{def}(t)$ before time t can be written as follows:

$$\begin{aligned} P_{def}(t) \equiv \mathbb{P}(\tau_{def} \leq t) = \mathbb{P}_{S_0}(\tau_B \leq t) = \\ = \mathbb{P}(\tau_b^{(\rho)} \leq t | X_0^{(\rho)} = x_0) \equiv \mathbb{P}_{x_0}(\tau_b^{(\rho)} \leq t)\,, \end{aligned} \tag{3.11}$$

where $\tau_b^{(\rho)} := \inf\{t \geq 0 : X_t^{(\rho)} = b\}$, $b = \mathsf{X}(B)$ and $x_0 = \mathsf{X}(S_0)$ are given by the inverse of F in (3.5). The survival probability $P_{surv}(t)$ can be written as follows:

$$\begin{aligned} P_{surv}(t) = 1 - P_{def}(t) = 1 - \mathbb{P}_{x_0}(\tau_b^{(\rho)} \leq t) = \\ = \mathbb{P}_{x_0}(t < \tau_b^{(\rho)} < \infty) = \mathbb{P}_{x_0}(\tau_b^{(\rho)} > t), \end{aligned} \tag{3.12}$$

since $\mathbb{P}_{x_0}(\tau_b^{(\rho)} = \infty) = 0$ in the case of the Confluent–U process where ∞ is a (non-attracting) natural boundary.

The CDF of the first-hitting time down $\tau_b^{(\rho)}$ is given by the discrete spectral expansion [13]:

$$\mathbb{P}_{x_0}(\tau_b^{(\rho)} \leq t) = 1 - \alpha_1 \frac{\mathcal{U}(\frac{\rho}{\alpha_1}, \mu+1, \kappa b)}{\mathcal{U}(\frac{\rho}{\alpha_1}, \mu+1, \kappa x_0)} \sum_{n=1}^{\infty} \frac{e^{-(\rho+\lambda_n)t}}{(\rho+\lambda_n)} \frac{\mathcal{U}(-\frac{\lambda_n}{\alpha_1}, \mu+1, \kappa x_0)}{\mathcal{U}_1(-\frac{\lambda_n}{\alpha_1}, \mu+1, \kappa b)}, \tag{3.13}$$

where $\lambda_n, n = 1, \ldots, \infty$, are positive eigenvalues, i.e., the positive roots of

$$\mathcal{U}(-\frac{\lambda_n}{\alpha_1}, \mu+1, \kappa b) = 0\,, \tag{3.14}$$

where $\mathcal{U}_1(a,b,z) \equiv \dfrac{\partial \mathcal{U}(a,b,z)}{\partial a}$. Since $S_t = \mathsf{F}(X_t^{(\rho)})$, where F is monotonic, the first-hitting time probabilities are simply related by:

$$\mathbb{P}_{S_0}(\tau_B \leq t) = \mathbb{P}_{x_0}(\tau_b^{(\rho)} \leq t), \quad b = \mathsf{X}(B), \quad x_0 = \mathsf{X}(S_0). \tag{3.15}$$

Consider the stock price process killed at level $B \geq 0$, with transition PDF $p_S^{(B)}(t; S_0, S)$. Note that for $B = 0$ we recover the transition PDF in (3.8), $p_S^{(0)}(t; S_0, S) = p_S(t; S_0, S)$. We have another useful relation between the transition PDF and the first-hitting time CDF:

$$\mathbb{P}_{S_0}(\tau_B \leq t) = 1 - \int_B^{\infty} p_S^{(B)}(t; S_0, S)\mathrm{d}S = 1 - \frac{e^{-\rho t}}{\hat{u}_\rho(\kappa x_0)} \int_b^{\infty} \hat{u}_\rho(\kappa x) p_X^{(b)}(t; x_0, x)\mathrm{d}x, \tag{3.16}$$

where function $\hat{u}_\rho(x)$ is given by (3.4). $p_X^{(b)}(t; x_0, x)$ is the transition PDF for the CIR X-diffusion $X_t \in (b, \infty)$ killed at a given level $b = \mathsf{X}(B)$, which is given by [13]:

$$\begin{aligned} p_X^{(b)}(t; x_0, x) = \frac{\pi\kappa e^{-\kappa x}(\kappa x)^\mu}{\Gamma(\mu+1)\sin(\pi(\mu+1))} \\ \times \sum_{n=1}^{\infty} \frac{e^{-\lambda_n t} \mathcal{M}(-\nu_n, \mu+1, \kappa b) \tilde{\mathcal{U}}(-\nu_n, \mu+1, \kappa x) \tilde{\mathcal{U}}(-\nu_n, \mu+1, \kappa x_0)}{\sin(\pi\nu_n)\tilde{\mathcal{U}}_1(-\nu_n, \mu+1, \kappa b)}, \end{aligned} \tag{3.17}$$

where $\nu_n = \lambda_n/\alpha_1$, $\tilde{\mathcal{U}}(-a,b,z) = \dfrac{\sin(\pi b)}{a\Gamma(a)}\mathcal{U}(-a,b,z)$ and $\tilde{\mathcal{U}}_1(-a,b,z) = \dfrac{\sin(\pi b)}{a\Gamma(a)}\mathcal{U}_1(-a,b,z)$ are the scaled confluent hypergeometric function and its scaled partial derivative w.r.t. argument a, respectively. The eigenvalues $\{\lambda_n\}_{n\geq 1}$ are the same as above.

We note that the integral $\int_B^\infty p_S^{(B)}(t;S_0,S)\mathrm{d}S$ represents the survival probability before time t. Therefore, the default and survival probabilities are related to the transition density $p_S^{(B)}(t;S_0,S)$ and the barrier level B. Recent studies in credit derivatives pricing using structural approaches to model default make different assumptions about how the default barrier function is determined. Some studies employ a specific functional form of the default boundary [27], [28], whereas the default boundary is primarily a function of asset volatility. Other studies [29] assume a more flexible setup featuring an arbitrary deterministic default boundary function. In order to incorporate a default barrier into the Confluent–U model, we propose the default barrier $B(t)$ to have a piecewise and time-wise form. The default time is generally given by (assuming $S_0 \geq B(0)$)

$$\tau_{def} := \inf\{t \geq 0 : S_t \leq B(t)\}.$$

In its simplest form we have a constant barrier $B(t) = B$, for all $t \geq 0$.

Let us compute default probabilities with a non-constant (i.e., piecewise constant) decreasing default barrier

$$B(t) = \sum_{i=1}^{N} B_i \mathbf{1}_{(t_{i-1},t_i]}(t)\,, \tag{3.18}$$

where B_i corresponds to the default level for the time interval $t_{i-1} < t \leq t_i$, $B(0) = B_1$, $t_0 = 0$, $B_1 \geq B_2 \geq \ldots$. Let $b_i = \mathsf{X}(B_i)$, $x_0 = \mathsf{X}(S_0)$. The default probabilities, i.e., the first-hitting time CDF for the S-diffusion across the piecewise constant barrier $B(t)$, can then be computed from first principles by concatenation. For up to $N = 2$, we have:

- for $0 < t \leq t_1$:

$$\mathbb{P}(\tau_{def} \leq t) = \mathbb{P}_{S_0}(\tau_{B_1} \leq t) = \mathbb{P}_{x_0}(\tau_{b_1}^{(\rho)} \leq t), \tag{3.19}$$

  where $\mathbb{P}_{x_0}(\tau_{b_1}^{(\rho)} \leq t)$ is given by (3.13).

- for $t_1 < t \leq t_2$:

$$\begin{aligned}
\mathbb{P}(\tau_{def} \leq t) &= 1 - \mathbb{P}_{S_0}(\tau_{def} > t) = 1 - \mathbb{P}_{S_0}(\inf_{0\leq u\leq t_1} S_u > B_1, \inf_{t_1<u\leq t} S_u > B_2) \\
&= 1 - \int_{B_1}^{\infty}\int_{B_2}^{\infty} p_S^{(B_1)}(t_1; S_0, S_1)\, p_S^{(B_2)}(t - t_1; S_1, S_2)\,\mathrm{d}S_2\,\mathrm{d}S_1 \\
&= 1 - \int_{B_1}^{\infty} p_S^{(B_1)}(t_1; S_0, S_1)\,\mathbb{P}_{S_1}(\tau_{B_2} > t - t_1)\,\mathrm{d}S_1 \\
&= 1 - \int_{B_1}^{\infty} p_S^{(B_1)}(t_1; S_0, S_1)[1 - \mathbb{P}_{S_1}(\tau_{B_2} \leq t - t_1)]\,\mathrm{d}S_1 \\
&= 1 - \int_{B_1}^{\infty} p_S^{(B_1)}(t_1; S_0, S_1)\,\mathrm{d}S_1 + \int_{B_1}^{\infty} p_S^{(B_1)}(t_1; S_0, S_1)\mathbb{P}_{S_1}(\tau_{B_2} \leq t - t_1)\,\mathrm{d}S_1 \\
&= \mathbb{P}_{S_0}(\tau_{B_1} \leq t_1) + \int_{B_1}^{\infty} p_S^{(B_1)}(t_1; S_0, S_1)\mathbb{P}_{S_1}(\tau_{B_2} \leq t - t_1)\,\mathrm{d}S_1 \\
&= \mathbb{P}_{x_0}(\tau_{b_1}^{(\rho)} \leq t_1) + \frac{e^{-\rho t_1}}{\hat{u}_\rho(x_0)} \int_{b_1}^{\infty} \hat{u}_\rho(x) p_X^{(b_1)}(t_1; x_0, x)\mathbb{P}_x(\tau_{b_2}^{(\rho)} \leq t - t_1)\,\mathrm{d}x.
\end{aligned} \tag{3.20}$$

- for $t \geq t_2$:

$$\begin{aligned}
\mathbb{P}(\tau_{def} \leq t) &= \mathbb{P}(\tau_{def} \leq t_2) + \mathbb{P}_{S_0}(\inf_{0\leq u\leq t_1} S_u > B_1, \inf_{t_1<u\leq t_2} S_u > B_2, \inf_{t_2<u\leq t} S_u < B_3) \\
&= \mathbb{P}(\tau_{def} \leq t_2) \\
&+ \int_{B_2}^{\infty}\int_{B_1}^{\infty} p_S^{(B_1)}(t_1; S_0, S_1) p_S^{(B_2)}(t_2 - t_1; S_1, S_2)\mathbb{P}_{S_2}(\tau_{B_3} \leq t - t_2)\,dS_1\,\mathrm{d}S_2 \\
&= \mathbb{P}(\tau_{def} \leq t_2) \\
&+ \frac{e^{-\rho t_2}}{\hat{u}_\rho(x_0)} \int_{b_2}^{\infty} \left[\int_{b_1}^{\infty} \hat{u}_\rho(x_2) p_X^{(b_1)}(t_1; x_0, x_1) p_X^{(b_2)}(t_2 - t_1; x_1, x_2)\,\mathrm{d}x_1 \right] \\
&\times \mathbb{P}_{x_2}(\tau_{b_3}^{(\rho)} \leq t - t_2)\,\mathrm{d}x_2.
\end{aligned} \tag{3.21}$$

Note that in deriving (3.20) and (3.21) we have made use of the Markov property and the time homogeneity of the process.

3.2.1 Linkage to Intensity Based Default Models

According to the intensity based default model, the stochastic behavior of a default process is determined by a hazard rate function $h(t)$ for time $t \geq 0$ at which default events occur. Then, the instantaneous probability of default, conditional on having survived up to time t, is proportional to the product of the hazard rate $h(t)$ and the length of the infinitesimal time interval $\mathrm{d}t$: $\mathbb{P}[\tau_{def} \leq t + \mathrm{d}t | \tau_{def} > t] = h(t)\mathrm{d}t$. Integration gives the survival probability for a finite time interval as

$$P_{surv}(t) = \mathbb{P}(\tau_{def} > t) = e^{-\int_0^t h(u)\,\mathrm{d}u}. \tag{3.22}$$

Based on this representation for the survival probability, and assuming the constant default level B, the hazard rate $h(t)$ can be interpreted as

$$h(t) = -\frac{\mathrm{d}}{\mathrm{d}t}\ln P_{surv}(t) = -\frac{P'_{surv}(t)}{P_{surv}(t)} = \frac{\frac{\partial}{\partial t}\mathbb{P}_{x_0}(\tau_b^{(\rho)} \leq t)}{\mathbb{P}_{x_0}(\tau_b^{(\rho)} > t)}, \tag{3.23}$$

where $b = \mathsf{X}(B)$, $x_0 = \mathsf{X}(S_0)$. Substituting the (3.19) — (3.21) into (3.23) one can obtain hazard rate for the Confluent–U model with nonconstant default barrier levels. Let us define the density $p_b^{(\rho)}$ for the first-hitting time at default level b for the $X^{(\rho)}$-diffusion:

$$p_b^{(\rho)}(t;x) = \frac{\partial}{\partial t}\mathbb{P}_x(\tau_b^{(\rho)} \leq t) = \alpha_1 \frac{\mathcal{U}(\frac{\rho}{\alpha_1}, \mu+1, \kappa b)}{\mathcal{U}(\frac{\rho}{\alpha_1}, \mu+1, \kappa x_0)} \sum_{n=1}^{\infty} \frac{e^{-(\rho+\lambda_n)t}\mathcal{U}(-\frac{\lambda_n}{\alpha_1}, \mu+1, \kappa x_0)}{\mathcal{U}_1(-\frac{\lambda_n}{\alpha_1}, \mu+1, \kappa b)} \tag{3.24}$$

Then the hazard rate function for $0 \leq t \leq t_1$ with default barrier level B_1 has the following representation:

$$h(t) \equiv h(S_0, B_1, t) = \frac{\sum_{n=1}^{\infty} e^{-(\rho+\lambda_n)t}\mathcal{U}(-\frac{\lambda_n}{\alpha_1}, \mu+1, \kappa x_0)/\mathcal{U}_1(-\frac{\lambda_n}{\alpha_1}, \mu+1, \kappa b_1)}{\sum_{n=1}^{\infty} \frac{e^{-(\rho+\lambda_n)t}}{(\rho+\lambda_n)}\mathcal{U}(-\frac{\lambda_n}{\alpha_1}, \mu+1, \kappa x_0)/\mathcal{U}_1(-\frac{\lambda_n}{\alpha_1}, \mu+1, \kappa b_1)}, \tag{3.25}$$

where $\{\lambda_n\}_{n\geq 1}$ are given by (3.14), $b_1 = \mathsf{X}(B_1)$, $x_0 = \mathsf{X}(S_0)$. For $t_1 < t \leq t_2$ from (3.20) and (3.24) the hazard rate function is

$$h(t) = \frac{\frac{e^{-\rho t_1}}{\hat{u}_\rho(x_0)} \int_{b_1}^{\infty} \hat{u}_\rho(x) p_X^{(b_1)}(t_1; x_0, x) p_b^{(\rho)}(t - t_1; x)\,\mathrm{d}x}{\mathbb{P}_{x_0}(\tau_{b_1}^{(\rho)} \leq t_1) + \frac{e^{-\rho t_1}}{\hat{u}_\rho(x_0)} \int_{b_1}^{\infty} \hat{u}_\rho(x) p_X^{(b_1)}(t_1; x_0, x)\mathbb{P}_x(\tau_{b_2}^{(\rho)} \leq t - t_1)\,\mathrm{d}x}. \tag{3.26}$$

Similarly, one can obtain the hazard rate function for $t_2 < t$:

$$h(t) = \frac{\frac{e^{-\rho t_2}}{\hat{u}_\rho(x_0)} \int_{b_2}^{\infty}\int_{b_1}^{\infty} \hat{u}_\rho(x_2) p_X^{(b_1)}(t_1; x_0, x_1) p_X^{(b_2)}(t_2 - t_1; x_1, x_2) p_{b_3}^{(\rho)}(t - t_2; x_2)\, \mathrm{d}x_1\, \mathrm{d}x_2}{\mathbb{P}(\tau_{def} \le t_2) + \frac{e^{-\rho t_2}}{\hat{u}_\rho(x_0)} \int_{b_2}^{\infty}\int_{b_1}^{\infty} \hat{u}_\rho(x_2) p_X^{(b_1)}(t_1; x_0, x_1) p_X^{(b_2)}(t_2 - t_1; x_1, x_2) \mathbb{P}_{x_2}(\tau_{b_3}^{(\rho)} \le t - t_2)\, \mathrm{d}x_1\, \mathrm{d}x_2} \tag{3.27}$$

Figure 3.2 gives an example of different hazard rate curves obtained using (3.25). The parameters used are: $S_0 = 14.5, B = 5.8, a_0 = 12.5, \mu = 1.25, \alpha_1 = 0.1, \nu = 2, r = 0.02$. One advantage of formula (3.25) is that it allows us to calculate implied hazard rates and survival probabilities based on historical stock prices.

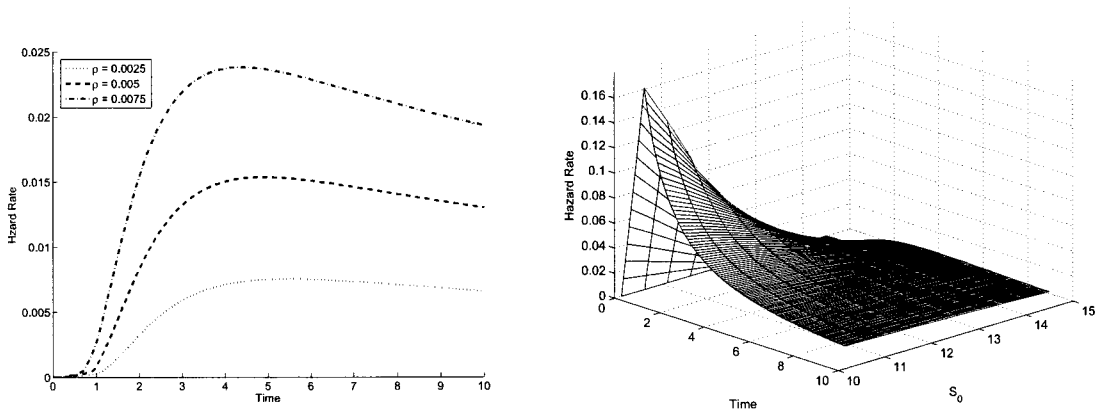

Figure 3.2: The term structure of hazard rates per annum for different values of ρ (left plot). The term structure of hazard rates per annum for varying spot price S_0 with $\rho = 0.005$ (right plot).

3.2.2 Matching Empirical Default Probabilities

For our first simple numerical example, we examine the ability of the Confluent–U default model to capture the actual average observed (real-world) default probabilities across bonds with different ratings. In our experiment, we use historical data derived from observations of default events captured between 1970 and 2000 in the report provided by Moody's in [30].

The Confluent–U model parameters $\xi = \{a_0, \mu, \alpha_1, \rho, \nu\}$, drift rate r and default barrier $B(t)$ were calibrated to fit the curve of the average historical cumulative default probabilities

for two types of bonds with investment grade and speculative grade ratings[1], respectively, with maturity of 10 years. The calibration procedure minimizes the least square error between the historical default probabilities and the default probabilities produced by the Confluent–U model using formulas (3.13), (3.17) — (3.21). It is assumed that the company's spot price S_0 is normalized and is equal to 100. We note that the same results are readily calibrated if one varies S_0. The following objective function is minimized:

$$\sum_{i=1}^{N} \left(P_{def}(t_i) - P_{def}^{obs}(t_i) \right)^2 \to \min_{\xi, B_{1,2,3}}, \tag{3.28}$$

where $t_i = i$, $i = 1, \ldots, 10$, $P_{def}^{obs}(t_i)$ corresponds to the observed default probability at t_i.

Figure 3.3 and 3.4 reports the numerical results of fitting the Confluent–U model to credit default rates from 1 to 10 years maturity for speculative and investment grade bonds, respectively. The optimal model parameters and default barrier levels are reported in Table 3.1. It is clear from these figures that the Confluent–U default model calibration matches default rates quite accurately over all time horizons and is capable of reproducing the general shapes of default probabilities for bonds with different ratings.

	a_0	μ	α_1	ρ	r	B_1	B_2	B_3
Investment Grade	94.23	1.995	0.087	0.0004	0.02	59.9	24.0	23.8
Speculative Grade	93.7	1.198	0.123	0.0112	0.051	52.2	41.5	40.85

Table 3.1: The optimal Confluent–U model parameters and default barriers obtained from the calibration for historical default probabilities for investment grade and speculative grade bonds. Note that parameter r in this case is the real-world growth rate.

[1]A bond is considered as investment grade if it is judged by the rating agency as likely enough to meet payment obligations that banks are allowed to invest in them. Speculative grade rating is below investment grade with higher risk of default.

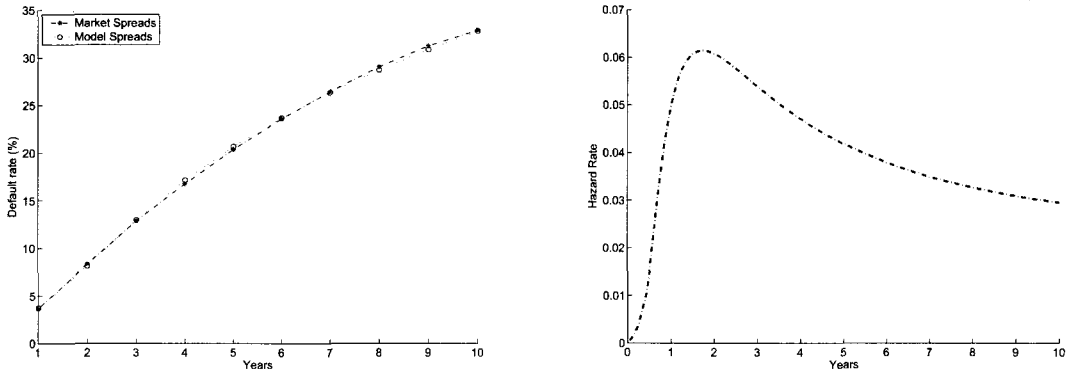

Figure 3.3: Confluent–U model default rates plotted against historical average default rates for the period from 1970 to 2000 for speculative grade bonds (left plot) and the respective hazard rate (right plot).

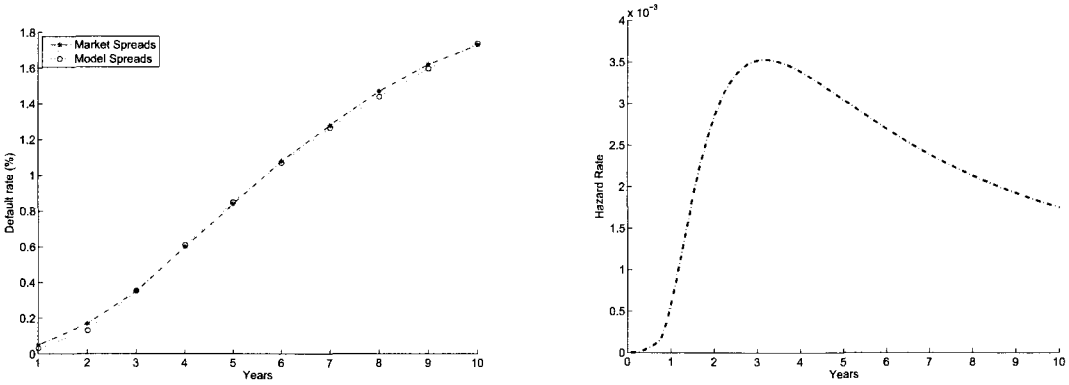

Figure 3.4: Confluent–U model default rates plotted against historical average default rates for the period from 1970 to 2000 for investment grade bonds (left plot) and the respective hazard rate (right plot).

3.2.3 Pricing Bond Spreads

Consider a defaultable zero-coupon bond with unit notional value at maturity. The payoff $Z_R(T)$ with maturity T and recovery rate R is given by:

$$Z_R(T) \equiv Z_R(S_0, T) = \mathbf{1}_{\{\tau > T\}} + R\mathbf{1}_{\{\tau \leq T\}} = (1 - R)\mathbf{1}_{\{\tau > T\}} + R, \tag{3.29}$$

where $\tau = \tau_{def}$ is a default time. For constant risk-free discount rate r and constant recovery rate R, spot price S_0, the current price of a defaultable zero-coupon bond maturing at T is:

$$P_R(S_0, T) = e^{-rT}\mathbb{E}_{S_0}\left[Z_R(T)\right] = e^{-rT}R + (1-R)e^{-rT}\mathbb{P}_{S_0}(\tau > T). \tag{3.30}$$

Assuming that the event of default occurs when the stock price falls below level B, $0 \leq B < S_0$, then $P_R(B, S_0, T)$ is the price of a defaultable zero-coupon bond with default barrier B:

$$\begin{aligned} P_R(S_0, T; B) &= e^{-rT}R + (1-R)e^{-rT}\mathbb{P}_{S_0}(\tau_B > T) && (3.31) \\ &= e^{-rT}R + (1-R)e^{-rT}(1 - \mathbb{P}_{S_0}(\tau_B \leq T)). && (3.32) \end{aligned}$$

Bond prices can be quoted as credit spreads over treasury bond yields due to different credit quality. Let $y(T)$ be the present risk-free treasury yield curve, then the bond credit spreads are given by:

$$s_R(S_0, T; B) = -\frac{1}{T}\ln P_R(S_0, T; B) - y(T). \tag{3.33}$$

Figures 3.5 and 3.6 illustrate some typical shapes of the term structure of bond credit spreads quoted in bps (a basis point (bp) is equal to 1/100th of 1%) for the model considered above as one varies the model parameters, including the single default barrier level B. The spot price is $S_0 = 14.5$, the risk-free rate is taken to match the yield curve of the US Treasury for December 6, 2009 and is provided in Table 3.3. Each figure contains four curves corresponding to four choices of model parameters. Fixed values of the parameters and their ranges are shown in Table 3.2.

As usual in no-arbitrage pricing the price of a CDS is given by the risk neutral expectation of its discounted payoff.

3.2.4 Pricing Credit Default Swaps

A Credit Default Swap (CDS) is a contract that provides insurance against the risk of a default by a particular company (the reference entity). The protection buyer regularly pays

Parameter	B	a_0	μ	α_1	ρ
Fixed value	5.8000	12.5181	1.2177	0.0939	0.0075
Min value	2	8	0.001	0.0100	0.001
Max value	8	15	4.5	0.5	0.01

Table 3.2: The model parameters and their ranges.

Period	3 mo	3 mo	1 yr	2 yr	3 yr	5 yr	7 yr	10 yr
Rate (%)	0.06	0.17	0.36	0.84	1.34	2.24	2.97	3.48

Table 3.3: US Treasury bond yields for December 6, 2009.

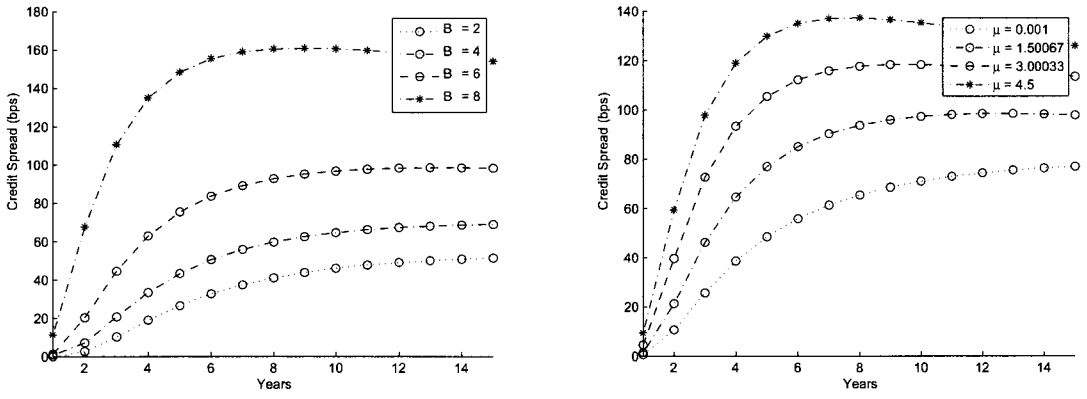

Figure 3.5: Some representative term structures of credit spreads with varying parameter B (left plot) and μ (right plot).

a stream of constant premiums to the protection seller until the maturity of the CDS t_N or the default time τ if $\tau < t_N$. The premium paid by the protection buyer to the seller is called the spread and is quoted in basis points per annum of the notional value of the contract and is usually paid quarterly.

Without loss in generality, we assume that there are N contractual payment dates $t_1 < t_2 < \cdots < t_N$ between the current time $t \leq t_1$ and the maturity at $T = t_N$. So, the payment at time $t_i \leq t_N, i = 1, \ldots, N$, is made only if $\tau > t_i$. Then the value of the

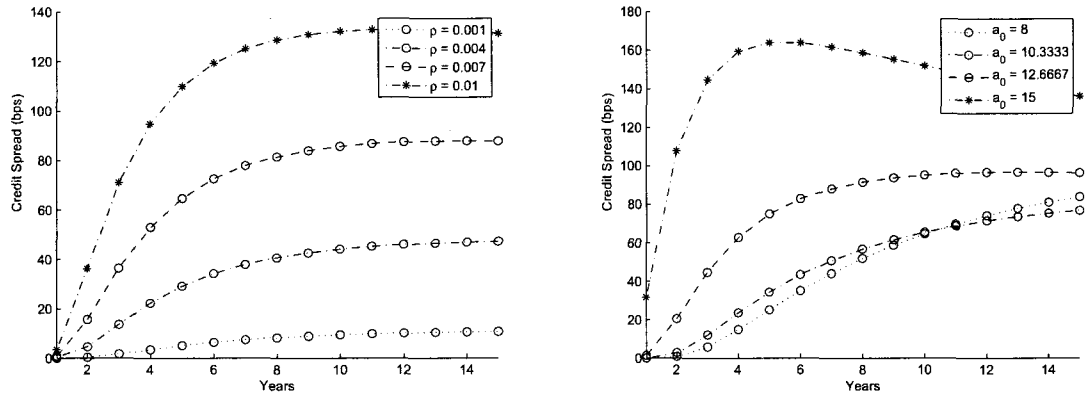

Figure 3.6: Typical term structures of credit spreads with varying parameter ρ (left plot) and a_0 (right plot).

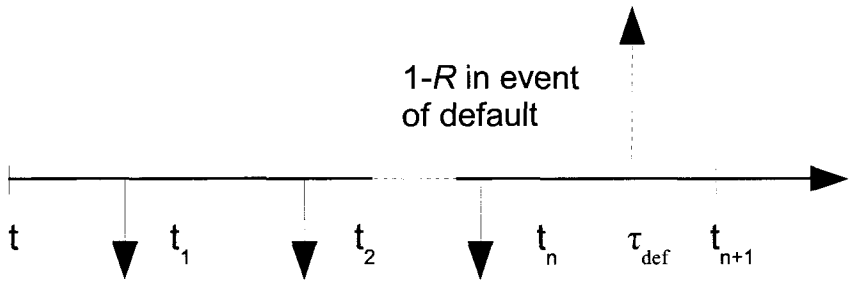

Figure 3.7: CDS contract cash flows.

premium leg at time t is equal to

$$s(t_N) \sum_{i=1}^{N} D(t, t_i) a_i \mathbf{1}_{\{\tau > t_i\}} ,$$

where $s(t, t_N) \equiv s(t_N)$ is the t_N-maturity contractual default swap spread, $D(t, T) = M(t)/M(T)$ is the discount factor at time t for maturity $T \geq t$, where $M(t)$ denotes risk-free money market account (i.e., bank account) numeraire, i.e., $M(t) = e^{\int_0^t r(s)\mathrm{d}s}$; $a_i = t_i - t_{t-1}$ is the year fraction between payment dates t_i and t_{t-1}.

If the reference entity defaults before the end of the CDS contract maturity $T = t_N$, then the protection seller pays to the protection buyer an amount $(1 - R)$, where $R \in [0, 1]$ is the recovery rate of the notional value (taken as \$1) which is delivered to the protection buyer at the default time, i.e., given default time τ, the amount delivered has present value

at time t

$$(1-R)D(t,\tau)\mathbf{1}_{\{t<\tau\leq t_N\}}.$$

For a par spread, the no-arbitrage present value, at time t, of the difference between the premium leg and the protection leg must equal zero, i.e.,

$$\mathbb{E}[(1-R)D(t,\tau)\mathbf{1}_{\{t<\tau\leq t_N\}} - s(t_N)\sum_{i=1}^{N} D(t,t_i)a_i\mathbf{1}_{\{\tau>t_i\}}|\mathcal{F}_t] = 0\,,$$

where this expectation is taken w.r.t. the risk-neutral equivalent martingale measure and the filtration $\mathcal{F}_t$ represents all available information up to time t, i.e., $\mathcal{F}_t = \sigma(S_u : 0 \leq u \leq t)$ is taken as the natural filtration generated by the stock price process. Then the expression for the par CDS spread $s(t_N)$ is given by

$$s(t_N) = \frac{(1-R)\int_t^{t_N} D(t,u)\mathrm{d}P_{def}(u)}{\sum_{i=1}^{N} D(t,t_i)a_iP_{surv}(t_i)} = \frac{(1-R)\int_t^{t_N} D(t,u)\mathrm{d}\mathbb{P}(\tau_{def}<u)}{\sum_{i=1}^{N} D(t,t_i)a_i\mathbb{P}(\tau_{def}>t_i)}\,, \tag{3.34}$$

where P_{surv} and P_{def} are the cumulative survival and default probabilities, respectively.

3.3 Calibration for CDS Spread Prices

The Confluent–U model is calibrated for CDS spreads with maturity ranging from 1 to 10 years for 4 publicly traded companies. To assess the capability of the Confluent–U model to adapt to different scenarios, the model is tested on the market CDS data for companies with various credit qualities. Sample data consist of closing CDS spread mid prices obtained from a Bloomberg terminal on February 16th, 2010. Figure (3.8) shows that observed companies produce different CDS spread curves. The following companies are considered:

- Apache — energy sector — "A+" S&P rating. The spot price is $S_0 = 91.2$.
- Walmart — retail sector — "AA" S&P rating. The spot price is $S_0 = 53.56$.
- Dell — technology sector — "A-" S&P rating. The spot price is $S_0 = 14.5$.
- Motorola — technology sector — "BB+" S&P rating. The spot price is $S_0 = 7.26$.

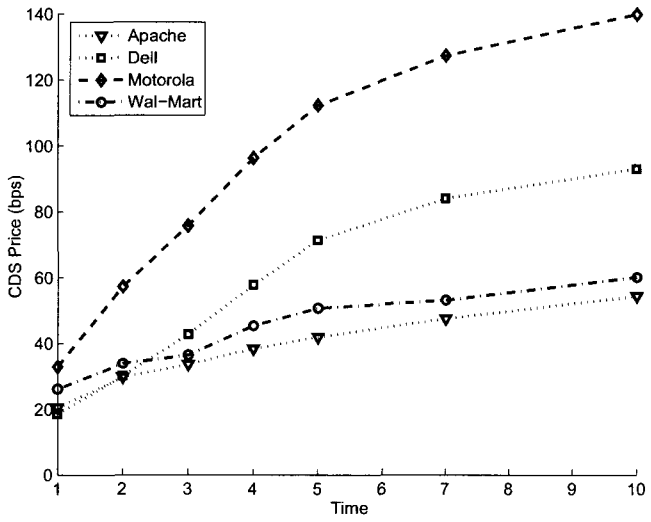

Figure 3.8: Market CDS spread curves for Dell, Apache, Motorola and Walmart.

The calibration procedure minimizes the sum of squares of the error between the market CDS spreads and the model CDS spreads, with respect to the given model parameter set ξ. Market CDS spreads are taken yearly from 1 to 10 years. The following objective function is considered:

$$F(\xi) = \sum_{i=1}^{N} w_i \left(s(t_i) - s_i(\xi)\right)^2 \rightarrow \min_{\xi}, \tag{3.35}$$

where $s(t_i), i = 1, 2, \ldots, N = 10$ are the observed market CDS spreads with t_i maturity, $s_i(\xi)$ are CDS spreads produced by the Confluent–U equity model according to the formula (3.34) with model parameters ξ, adjustable default barrier $B(t)$, and where w_i is the ith weight assigned to the ith data point.

3.3.1 Constant Default Barrier

In preparation for the non-constant default barrier calibration, for the first preliminary stage of the calibration it is assumed that the default barrier is constant, i.e., we simply set $B(t) = B$. The weights in the objective function are set to zero for the CDS spreads with

maturity less than 3 years, assuming that the default barrier for maturities $t_i \geq 3$ years is approximated by a constant value B.

The recovery rates are obtained from [31], which provides average recovery rates by industry for the period from 1982 to 2003. The recovery rates of $R = 25.5\%$, 34.8% and 53.4% are utilized for companies from technology, retail and energy sectors respectively. The risk-free discount rate is set to the US Treasury yield curve. The calibration procedure is the same for each company, thus all the steps of the calibration are shown below in detail only for the case of Dell.

The objective function (3.35) depends on the 5 model parameters (indicating the barrier level B) listed in Table 3.4. The objective function is minimized by using a gradient based algorithm. Calibration results are very sensitive to the initial set of parameters listed in Table 3.4. In order to recover an optimal parameter set for the Dell CDS data set, the initial guess for the default barrier B is varied from 0.5 to 13 with step size 0.25. For each default barrier the calibration algorithm provides an optimal set of parameters and the respective value of the objective function. The best solution with the minimal objective function is reported in Table 3.4.

Parameter	B	a_0	μ	α_1	ρ
Lower bound	0.5	0.1	0.0001	0.01	0.00001
Upper bound	13	25	4.5	0.5	0.5
Initial value	5	13.5	1.25	0.1	0.001
Optimal value	1.851	12.806	0.177	0.1229	0.0128

Table 3.4: Model parameters, their boundaries, initial guess and optimal values.

Figure 3.9 plots the comparison between the model and the market CDS spreads. Our results show that for a constant default level $B = 1.85$ the Confluent–U model can produce an excellent fit to the CDS spreads with maturity from 3 to 10 years, i.e., for data points with maturity ≥ 3 years.

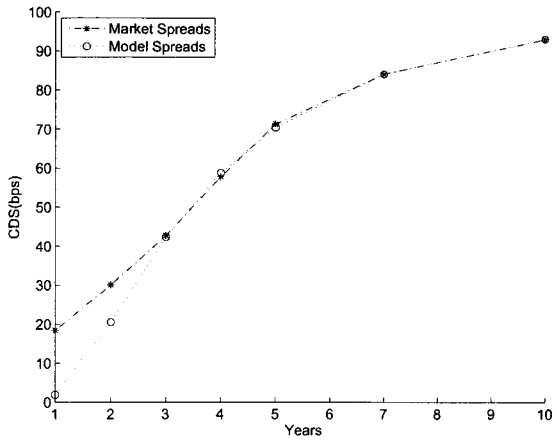

Figure 3.9: Market CDS spreads for Dell company and spreads produced by Confluent–U model with a constant default barrier.

3.3.2 Piecewise Default Barrier

To minimize the overall error in the CDS curve, as well as, the error between market and model CDS spreads with maturity < 3 years (i.e., for the first and second years) a step-wise non-constant barrier is employed. However, a piecewise default level increases the computational time due to the necessity of computing a single and double integral in formula (3.21). For multiple barrier levels the model calibration involves multiple integrals. As a trade-off between the speed and accuracy, the default level is specified with only 3 segments as follows:

$$B(t) = \begin{cases} B_1, & 0 < t \leq 1, \\ B_2, & 1 < t \leq 2, \\ B_3, & 2 < t \leq 10. \end{cases}$$

Thus, the default level is non-constant for the first two years of the CDS spreads and is constant for the rest of the maturities. Steps 1–3 below constitute the algorithm that we have applied for the full CDS calibration.

Step 1. Obtain a preliminary estimate of $B_3 \cong \hat{B}_3^{(1)}$ by calibrating to CDS spreads for maturity ≥ 3 years.

(i) Set $w_1 = w_2 = 0$ in equation (3.35).

(ii) Use formula (3.19) and (3.13) to compute the default probability for constant barrier B_3.

(iii) Obtain first estimates of $\xi \cong \hat{\xi}^{(1)}$ and $B_3 \cong \hat{B}_3^{(1)}$ by solving the optimization problem (3.35).

Step 2. Obtain a preliminary estimate of $B_2 \cong \hat{B}_2^{(1)}$ and an improved estimate of $B_3 \cong \hat{B}_3^{(2)}$ by calibrating CDS spreads for maturity ≥ 2 years.

(i) Set $w_1 = 0$ in equation (3.35).

(ii) As an initial guess, set model parameters and the two barrier levels to $\tilde{\xi} = \hat{\xi}^{(1)}, \{\tilde{B}_2, \tilde{B}_3\} = \{\hat{B}_3^{(1)}, \hat{B}_3^{(1)}\}$.

(iii) Use formulae (3.19) and (3.20) for the default probability for a two-step barrier.

(iv) Obtain estimates $\xi \cong \hat{\xi}^{(2)}$ and $\{B_1, B_2\} \cong \{\hat{B}_2^{(1)}, \hat{B}_3^{(2)}\}$ by solving the optimization problem (3.35).

Step 3. Obtain the final estimates of the set of parameters ξ and the piecewise constant default barrier$\{B_1, B_2, B_3\}$ by calibrating to CDS spreads for the whole range of maturities.

(i) As an initial guess, set model parameters to $\tilde{\xi} = \hat{\xi}^{(2)}$, $\{\tilde{B}_1, \tilde{B}_2, \tilde{B}_3\} = \{\hat{B}_2^{(1)}, \hat{B}_2^{(1)}, \hat{B}_3^{(2)}\}$.

(ii) Use the formulae (3.19)—(3.21) for the default probability for the case of the three-step piecewise barrier.

(iii) Finally, obtain the calibrated model parameters ξ and compute the default barrier $\{B_1, B_2, B_3\}$ by solving the optimization problem (3.35).

The results in Figure 3.10 show that the calibration with a piecewise default level produces a significantly better fit to the market spreads than the constant barrier calibration.

The optimal non-constant default levels are $B_1 = 7.26, B_2 = 2.72, B_3 = 1.89$, and the optimal model parameters are $a_0 = 12.883, \mu = 0.173, \alpha_1 = 0.117, \rho = 0.0126$.

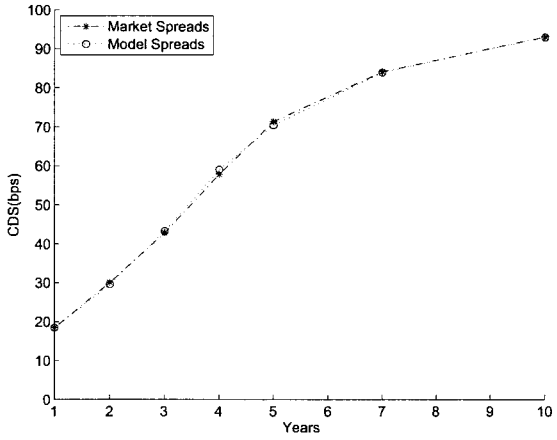

Figure 3.10: Comparison of market and model CDS spreads for Dell with the piecewise default level $B_1 = 7.26, B_2 = 2.72, B_3 = 1.89$.

The above calibration procedure was also applied to Walmart, Motorola and Apache companies. The results of the calibrations are respectively reported in Figures 3.11, 3.12 and 3.13. Our results confirm that the Confluent–U default model can produce various shapes of the CDS spreads and works reasonably well, and in some cases exceptionally well, to fit market CDS data.

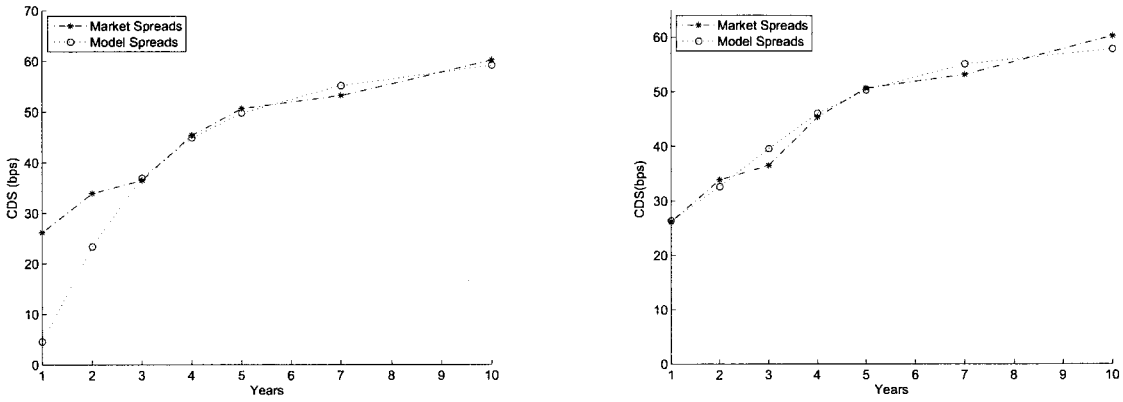

Figure 3.11: Calibration results for Walmart using a constant default barrier $B = 22.52$ (left plot) and three default barrier levels (right plot), where $B_1 = 40.11, B_2 = 22.88, B_3 = 22.31$.

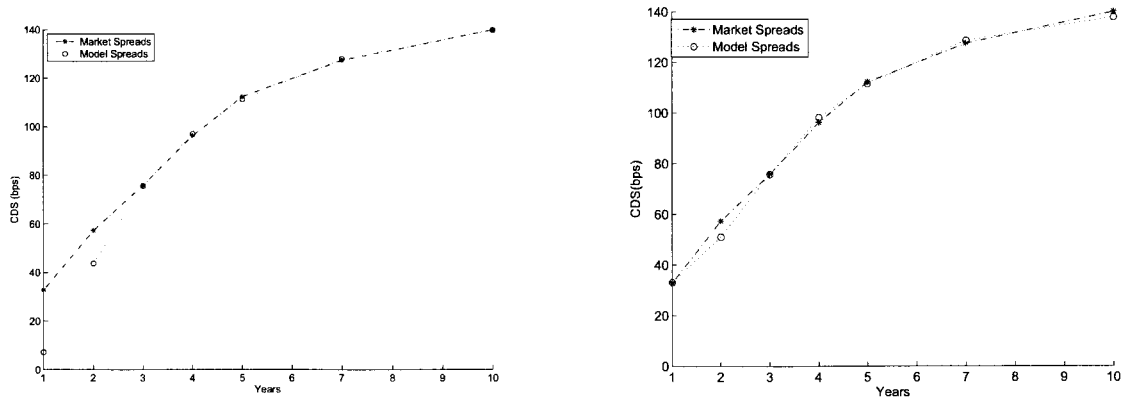

Figure 3.12: Calibration results for Motorola using a constant default barrier $B = 1.55$ (left plot) and three default barrier levels (right plot), where $B_1 = 3.25, B_2 = 1.59, B_3 = 1.51$.

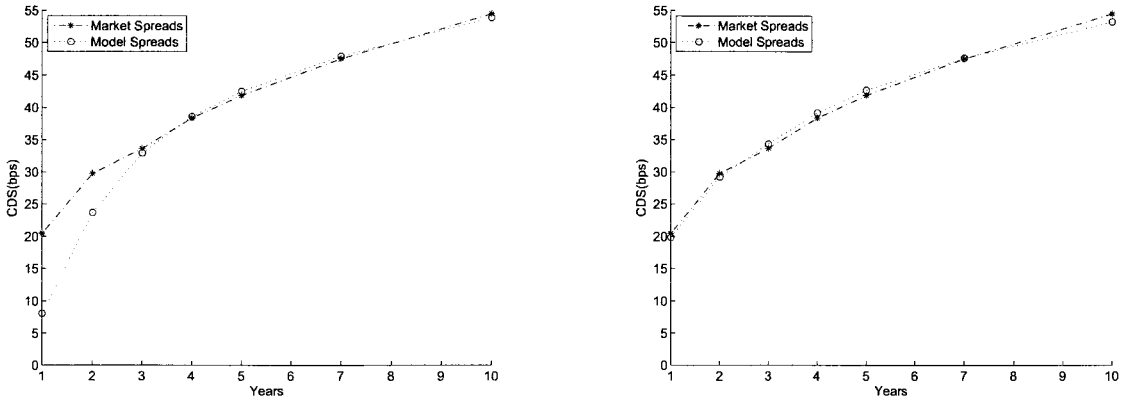

Figure 3.13: Calibration results for Apache using a constant default barrier $B = 11.85$ (left plot) and three default barrier levels (right plot), where $B_1 = 55.51, B_2 = 14.31, B_3 = 10.9$.

3.4 Linkage Between CDS Spreads and Put Options

Let us consider an investor who wants to protect long position in company stocks from default. Assuming a particular recovery rate, the same payoff of a CDS can be replicated with deep out-of-the-money put options. Assuming that an investor is looking for \$1 million worth of protection for the next year, the stock of Apache on April 14th, 2010 is trading at $S_0 = \$92.75$ and put option with strike $K = 40$ and expiration of one year has a mid-market price of \$0.63. The 5-year CDS contract spread is quoted as 41.8 bps.

Assuming a 40% recovery rate, the CDS would pay the protection buyer $\$600,000$ in the event of default. Assume that the event of default occurs when the stock price hits zero. The investor needs to purchase $600,000/(40 \times 100) = 150$ put contracts (1 contract consists of 100 puts) with 1 year maturity to obtain a $\$600,000$ payoff. The cost of this position would be $0.63 \times 150 \times 100 = \$9,450$. The cost of the same position in a CDS contract would be $\$4,128$ assuming continuous compounding with constant interest $r = 0.2\%$ per annum and 40% recovery rate. From this example we see that obtaining protection by entering into the put contract is much more expensive. However, one should take into account other factors such as liquidity and transaction costs. To adjust the price of protection and make it fair for put and CDS contracts, one should change the recovery rate to approximately 75%. This example raises an important question about the linkage between market CDS spreads and put options. This linkage is examined in Sections 3.4.1 and 3.4.2.

3.4.1 Calibration to Option Put Prices

We now consider the calibration procedure for the Confluent–U model for pricing European put options. Suppose we have N market prices of European put contracts
P_i, $i = 1, \ldots, N$. The calibration then consists of searching for the model parameter set of

values $\xi = \{\rho, a_0, \mu, \alpha_1, \theta\}$ that minimizes the objective function:

$$F(\xi, \xi_0; \gamma) = \sum_{i=1}^{N} w_i \left| P(K_i, T_i; \xi) - P_i \right|^2 + \gamma H(\xi, \xi_0) \to \min_{\xi} . \tag{3.36}$$

The objective function (3.36) consists of two terms. The first term incorporates pricing error between market option put prices P_i and model put option prices $P(K_i, T_i; \xi)$ with corresponding strike price K_i and maturity T_i. Here w_i are non-negative weights that reflect the relative importance of reproducing different put prices precisely.

The second component is a penalization term with regularization parameter γ and $H(\xi, \xi_0)$ as the relative entropy or the Kullback-Leibler distance (see Section 2.3.1):

$$H(\xi, \xi_0) = \mathbb{E}^{\mathbb{P}} \left[\ln \frac{d\mathbb{P}}{d\mathbb{P}_0} \right] . \tag{3.37}$$

With inclusion of the penalty term, the inverse problem becomes well-posed and measures the discrepancy between probability measure $\mathbb{P}$ with parameters ξ and a given prior measure $\mathbb{P}_0$ with parameter set ξ_0.

The choice of the prior probability density for the stock price process with parameters[2] $\xi_0 = \{\rho, a_0, \mu, \alpha_1, \theta\}$ is based on the result of the calibration of the Confluent–U model parameters to the time series of stock weekly returns for a one-year period. To evaluate the optimal parameter set ξ_0 with the best fit to the historical stock price data $\{S_1, \ldots, S_n\}$, the negative log-likelihood estimator has to be minimized:

$$\xi_0 = \arg\min_{\xi} \sum_{i=1}^{n} \left(-\ln p_S(\Delta t_i; S_{i-1}, S_i; \xi) \right),$$

where p_S is the transition PDF of the Confluent–U model given by formula (3.8). The historical data contain n weekly observations, i.e., $\Delta t_i = 1/52$, for a one year period for Apache from April 14th, 2009 to April 14th, 2010. The optimal parameter set is reported in Table 3.5.

[2]The drift parameter r has been replaced by θ as it now denotes the physical growth rate of the stock price.

a_0	μ	α_1	ρ	θ
83.48	1.684	0.493	0.0472	0.072

Table 3.5: Optimal model parameters ξ_0 obtained in the calibration for the historical prices.

To be able to estimate the performance of the Confluent–U model in terms of its ability to replicate the empirical density, it is compared to the Black–Scholes model. Taking into account that the Black-Scholes model assumes the log-normal distribution of stock returns, the expected growth rate $\hat{\theta}$ and volatility $\hat{\sigma}$ can be easily estimated:

$$\begin{aligned} \hat{\theta} &= \frac{\sum_{i=1}^{n} \log(\frac{S_i}{S_{i-1}})}{n}, \\ \hat{\sigma}^2 &= \frac{\sum_{i=1}^{n} [\log(\frac{S_i}{S_{i-1}}) - \hat{\theta}]^2}{n}. \end{aligned}$$

Once an optimal parameter set ξ_0 for the prior measure is obtained, the ratio of the likelihood estimators for the Confluent–U, MLE_U, and the Black-Scholes model, MLE_{BS}, is analyzed. For given $n = 48$ weekly historical observations for Apache from April 14th, 2009 to April 14th, 2010, the ratio MLE_{BS}/MLE_U is equal to 0.96. Hence, the Confluent–U model provides better fit to the historical data. We note that the Confluent–U model can capture more rare events in the fatter tails of the probability distribution.

The regularization parameter γ in (3.36) is estimated based on the Morozov discrepancy principle [7], which is described by the following algorithm:

1. Compute parameters of $\xi = \{\rho, a_0, \mu, \alpha_1\}$ (note $\theta = r$ in this step) by solving the nonlinear least squares problem (3.36) in low precision without penalty function.

2. Fix $\delta \in (1, 1.5)$ and numerically solve equation $F(\xi, \xi_0; \gamma) = \delta F(\xi, \xi_0; 0)$ for the regularization parameter γ, where $F(\xi, \xi_0; \gamma)$ is defined in (3.36).

The solution to the nonlinear least square problem with low precision is reported in Table 3.6. For given $\delta = 1.2$, the regularization parameter γ is equal to 2.3.

a_0	μ	α_1	ρ	r
86.158	1.5771	0.227	0.0546	0.0025

Table 3.6: Optimal model parameters obtained in the calibration for the option prices with low precision.

Solution to the nonlinear least squares problem (3.36) with regularization parameter γ and prior measure ξ_0 is estimated by a gradient-based method. The optimal parameter set is reported in Table 3.7.

a_0	μ	α_1	ρ	r
83.0651	1.87238	0.243	0.0563	0.0025

Table 3.7: Optimal model parameters obtained in the calibration for the put option prices.

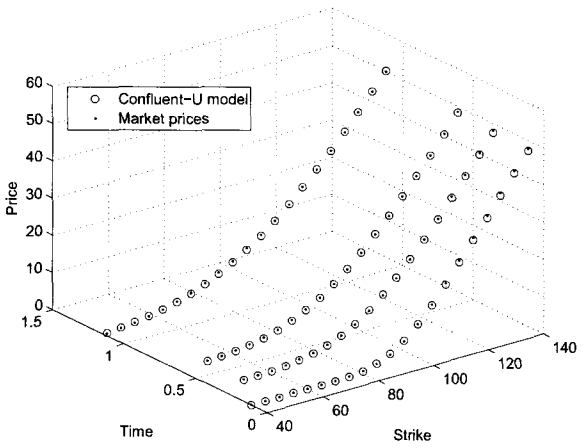

Figure 3.14: Comparison of market put option prices and Confluent–U model option prices.

In Figures 3.14, 3.15 and 3.16 the results of the calibration to option put prices are reported. It is clear from the results that the Confluent–U model can be calibrated with a very good fit to option prices for various range of maturities and strikes.

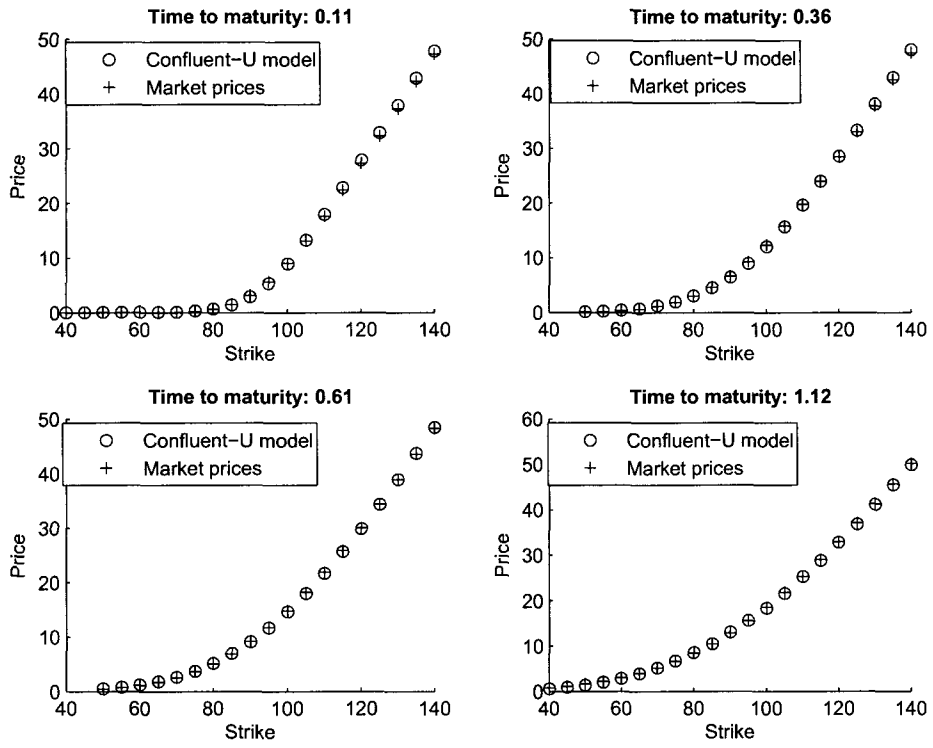

Figure 3.15: Comparison of market put option prices and Confluent–U model option prices for different maturities in years.

3.4.2 Pricing CDS Based on Confluent–U Model Calibrated to Put Options

To link the European put options to the CDS spreads on the same reference company, we assume that the recovery rate R and default barrier B are unknown. The CDS quotes are obtained from Bloomberg on April 14th, 2010 for Apache company. To empirically test the strength of the linkage between the European put options and CDS spreads, we price CDS spreads by formula 3.34. The Confluent–U model parameters set correspond to results of calibration to put option prices and are shown in Table 3.7. Recovery rate R and default barrier B are calibrated to the fit the model to curve of market CDS data. The calibration procedure described in details in Section 3.3. The results of calibration

Market prices	Model prices	Abolute error	Relative error (%)
0.52	0.47	0.05	10.24
0.80	0.74	0.06	7.47
1.25	1.15	0.10	8.32
1.85	1.73	0.12	6.46
2.65	2.55	0.10	3.88
3.75	3.65	0.10	2.63
5.20	5.09	0.11	2.03
7.00	6.92	0.08	1.20
9.10	9.14	0.04	0.44
11.70	11.77	0.07	0.59
14.65	14.79	0.14	0.94
18.00	18.17	0.17	0.92
21.70	21.86	0.16	0.73
25.70	25.82	0.12	0.48
29.90	30.01	0.11	0.37
34.35	34.38	0.03	0.08
38.95	38.89	0.06	0.15
43.70	43.52	0.18	0.42
48.45	48.23	0.22	0.45

Figure 3.16: Comparison of market put option prices and Confluent–U model option prices for maturity $T = 0.61$.

are reported in Figure 3.17, where computed CDS curves are plotted against market CDS spreads. The obtained recovery rate is equal to 91.1%, default level is $B(t) = \{B_1 = 20.08, B_2 = 7.62, B_3 = 0.49\}$.

We observe that the Confluent–U model calibration matches CDS curve quite accurately over all time horizons. One can investigate time series of the CDS spreads and options prices to determine correlation of co-movements and predict future movements in both

markets. This information can be used to identify arbitrage opportunities and, hence, can be incorporated in trading strategies. We conclude that one can examine more about the CDS and the stock options markets to determine more accurate relationship between credit and market risk. Note, that Confluent–U model allows us to integrate both markets, rather than to utilize separate models for each market.

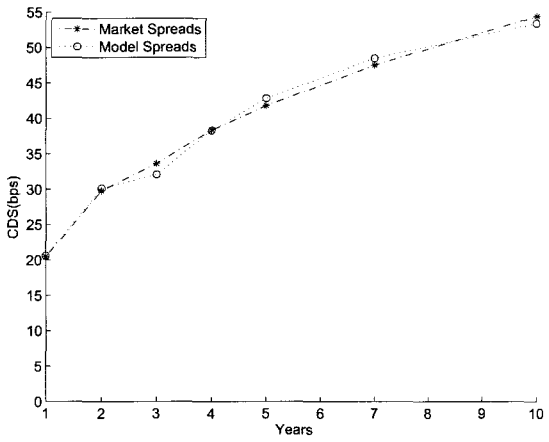

Figure 3.17: CDS spreads implied from calibration to put options against market CDS spreads for mid quoted prices for Apache on April 16th, 2010.

Conclusion

In this thesis we have studied two separate sets of problems that are of considerable importance in mathematical finance from both the theoretical and practical viewpoints. The first main problem consisted of formulating a new model for describing multi-asset price dynamics that can be readily calibrated realistically to market implied volatility surfaces for option prices on a single stock while also incorporating historical correlations among multiple stocks. The other main problem consisted of developing a new equity-based structural model for simultaneously pricing credit default swap (CDS) spreads and standard European equity call/put options on a given firm and then linking the two results.

The mathematical framework underlying the single stock price dynamics is the so-called diffusion canonical transformation for constructing solvable multi-parameter nonlinear local volatility diffusion models with affine drift [15], [10]. In particular, the models and applications considered in this thesis specialize to two main families of recently developed nonlinear local volatility models: one is the UOU model that is generated by taking the standard Ornstein–Uhlenbeck (OU) diffusion as underlying process while the other is the Confluent–U family which is built on the Cox–Ingersoll-Ross (CIR) (or Feller) process. The forward price (i.e. discounted price) process for all such models is a martingale under a given risk-neutral measure. The transition probability densities, as well as the probability distributions and densities for other relevant quantities such as first hitting times, for such models are given in analytically closed form in terms of known special functions, namely confluent hypergeometric functions. The martingale property of the discounted processes allowed us to apply an arbitrage-free risk-neutral asset pricing methodology. We also showed that these models produce curves for the local volatility function that have a wide range of pronounced smiles and skews of the type observed in the option markets. In fact, we have successfully calibrated the above models to different sets of observed market equity option data and showed good quantitative agreement between the model and observed European option prices for a wide range of strikes and maturities.

In the first part of the thesis, the multivariate UOU process with built-in correlations was constructed by using a copula function, where independent Ornstein–Uhlenbeck processes are coupled by employing a bridge copula method. We presented a computational implementation of the bridge and sequential simulation algorithm for the multivariate UOU asset price process. To illustrate the applicability of the UOU model for financial applications, we successfully calibrated the model to standard equity option market prices using data from four different firms. As well, the model was readily calibrated to provide a fit to a multi-stock price correlation matrix, for the four firms, by using historical stock prices.

Since the calibration procedure dealt with an ill-posed inverse problem, we applied a regularization method based on relative entropy with respect to the historical prior measure. The prior measure was obtained by applying a maximum likelihood estimator technique to the historical observation of the stocks returns. Mainly, the calibration procedure employed nonlinear least squares to find optimal model parameters. The calibration procedure for the multivariate case involved computation of the optimal correlation matrix. However, the resulting matrix could violate the positive definite property of a correlation matrix. To overcome this problem, we applied a method of spectral decomposition. In the second main part of the thesis, we introduced an equity-based structural first-passage time default framework in which stock prices are modeled according to the Confluent–U family of diffusion models. The model admits very efficient closed-form formulas for default probabilities that incorporate freely adjustable non-constant default barrier levels. By fitting the Confluent–U model to the historical data derived from observations of default events, we demonstrated its ability to accurately capture average observed default probabilities across bonds with different ratings and up to a maturity of ten years. We demonstrated how to link our equity barrier default model to an intensity based default model: our Confluent-U model allows us to calculate implied hazard rates across all maturities. We also tested the model robustness by calibrating it to some market CDS spreads for companies with various credit ratings across various sectors. We showed that the model with piecewise default barrier level is readily and accurately calibrated to the credit spreads. Finally, our equity-based default model provides a natural framework for simultaneously handling both equity option pricing and CDS pricing since one can employ various calibration schemes for the volatility parameters, the default levels, and the recovery rate in the model. In particular, by calibrating to CDS spread data, the model provides predictability for equity option prices and vice versa if one instead calibrates the model to option prices. Based on this fact, we can investigate the linkage between CDS spreads and out-of-the-money put options as a source of protection from the credit default of a firm.

The encouraging results of the model calibrations and applications in this thesis pave the way to further study of such solvable models. The successful applications of the nonlinear local volatility diffusion models to financial modeling presented in this paper naturally raise further practical and academic interest in these models. The availability of analytically closed form expressions for the transition probability densities and first-hitting time probabilities allow us to employ further extensions and to further improve upon such solvable diffusion models. One such avenue of model extensions may involve the incorporation of stochastic time changes. Another is the additional inclusion of an instantaneous killing (hazard) rate in the solvable diffusion process.

References

[1] Bachelier L. *The Theory of Speculation.* PhD thesis, 1900.

[2] Samuelson P. Rational theory of warrant pricing. *Industrial Management Review*, 1965.

[3] Steven Heston. A closed-form solution for options with stochastic volatility with applications to bond and currency options. *Review of Financial Studies*, 1993.

[4] John Hull and Allan White. The pricing of options with stochastic volatilities. *Journal of Finance*, 1987.

[5] Robert Merton. Option pricing when underlying stock returns are discontinuous. *Journal of Financial Economics*, 1976.

[6] Andersen L. and Andreasen J. Jump-diffusion processes: volatility smile fitting and numerical methods for option pricing. *Review of Derivative Research*, 2000.

[7] Cont R. and P. Tankov. *Financial Modelling with Jump Processes.* Chapman and Hall/CRC, 2004.

[8] Dupire B. Pricing with a smile. *RISK magazine*, 1994.

[9] Cox J.C. and S. Ross. The valuation of options for alternative stochastic processes. *Journal of Financial Economics*, 1976.

[10] Albanese C., G. Campolieti, P. Carr, and A. Lipton. Black-scholes goes hypergeometric. *Risk*, 2001.

[11] Campolieti G. and R. Makarov. On properties of some analytically solvable families of local volatility diffusion models. *Revised version accepted*, Feb 2010.

[12] Campolieti G., R. N. Makarov, and A. Vasiliev. Bridge copula method for multi-asset pricing. *Submitted to International Journal of Theoretical and Applied Finance*, 2009.

[13] Campolieti G. Closed-form spectral expansions: Fist hitting time distributions and transition densities for new families of killed diffusions. *Working paper*, 2008.

[14] Campolieti G. and R. Makarov. Solvable nonlinear volatility diffusion models with affine drift. Quantitative Finance Papers 0907.2926, arXiv.org, July 2009.

[15] Albanese C. and G. Campolieti. *Advanced Derivatives Pricing and Risk Management: Theory, Tools, and Hands-on Programming Applications.* Elsevier Academic Press, New York, NY, USA, 2005.

[16] Borodin A.N. and P. Salminen. *Handbook of Brownian Motion – Facts and Formulae.* Birkhauser, 2002.

[17] Abramowitz M. and I.A. Stegun. *Handbook of Mathematical Functions.* Dover, New York, 1972.

[18] Nelsen R. *An Introduction to Copulas.* New York, 1999.

[19] Engl H.W., M. Hanke, and A. Neubauer. *Regularization of Inverse Problems.* Kluwer Academic Publishers, Dordrecht, 1996.

[20] Jaeckel P. and R. Rebonato. The most general methodology for creating a valid correlation matrix for risk management and option pricing purposes. *Journal of Risk*, 1999/2000.

[21] John C Cox, Jr Ingersoll, Jonathan E, and Stephen A Ross. A theory of the term structure of interest rates. *Econometrica*, 53(2):385–407, March 1985.

[22] Fischer Black and Myron S Scholes. The pricing of options and corporate liabilities. *Journal of Political Economy*, 81(3):637–54, May-June 1973.

[23] Robert C. Merton. On the pricing of corporate debt: The risk structure of interest rates. *The Journal of Finance*, 29(2):449–470, 1974.

[24] Jarrow Robert A and Stuart M Turnbull. Pricing derivatives on financial securities subject to credit risk. *Journal of Finance*, 50(1):53–85, March 1995.

[25] Vadim Linetsky. Pricing equity derivatives subject to bankruptcy. *Mathematical Finance*, 16(2):255–282, 2006.

[26] Peter Carr and Vadim Linetsky. A jump to default extended cev model: an application of bessel processes. *Finance and Stochastics*, 10(3):303–330, 2006.

[27] Brigo D. and M. Tarenghi. Credit default swap calibration and counterparty risk valuation with a scenario based first passage model. Quantitative Finance Papers 0912.3031, arXiv.org, December 2009.

[28] Brigo D. and M. Tarenghi. Credit default swap calibration and equity swap valuation under counterparty risk with a tractable structural model. Quantitative Finance Papers 0912.3028, arXiv.org, December 2009.

[29] Gregor Dorfleitner, Paul G. Schneider, and Tanja Veza. Flexing the Default Barrier. *SSRN eLibrary*, 2008.

[30] Moodys Investors Service. *Default & Recovery Rates of Corporate Bond Issuers.* 2000.

[31] Moodys Investors Service. *Recovery Rates on Defaulted Corporate Bonds and Preferred Stocks.* 2003.

[32] Albanese C. and Kuznetsov A. Unifying the three volatility models. *Risk Magazine*, 2004.

[33] Cont R. and P. Tankov. Financial modelling with jump processes. *Journal of the American Statistical Association*, 101:1315–1316, September 2006.

[34] Glasserman P. *Monte Carlo methods in financial engineering.* Springer-Verlag, New York, 2004.

[35] Hurd T.R. and Kuznetsov A. Explicit formulas for laplace transform of stochastic integrals. *Markov Process. Relat. Fields*, 14:303–330, 2008.

[36] John C. Hull. *Options, Futures, and Other Derivatives, 6th edition.* Prentice Hall, New York, NY, USA, 2005.

[37] Kuznetsov A. *Solvable Markov Processes.* PhD thesis, 2004.